

## CHAPTER 3

### Results

#### 3.1 UV-Vis spectroscopy

##### 3.1.1 Determining suitable concentration of curcumin

Suitable concentration of curcumin for spectrophotometric method was investigated by making series of curcumin at various concentrations ( $1.0 \times 10^{-6}$  -  $9.0 \times 10^{-5}$  M) and their absorptions were recorded as shown in Figure 18. The relation between concentration of curcumin in 50% MeOH and its maximum absorption at 430 nm are illustrated in Figure 19.

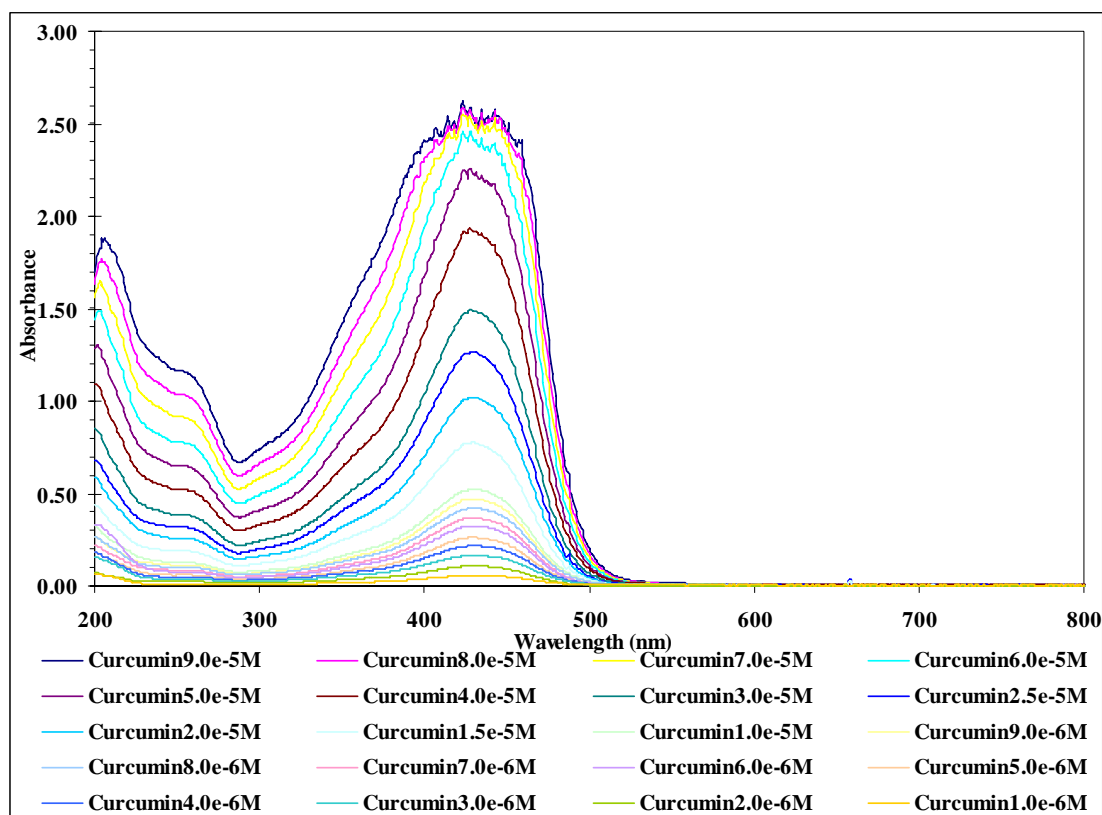
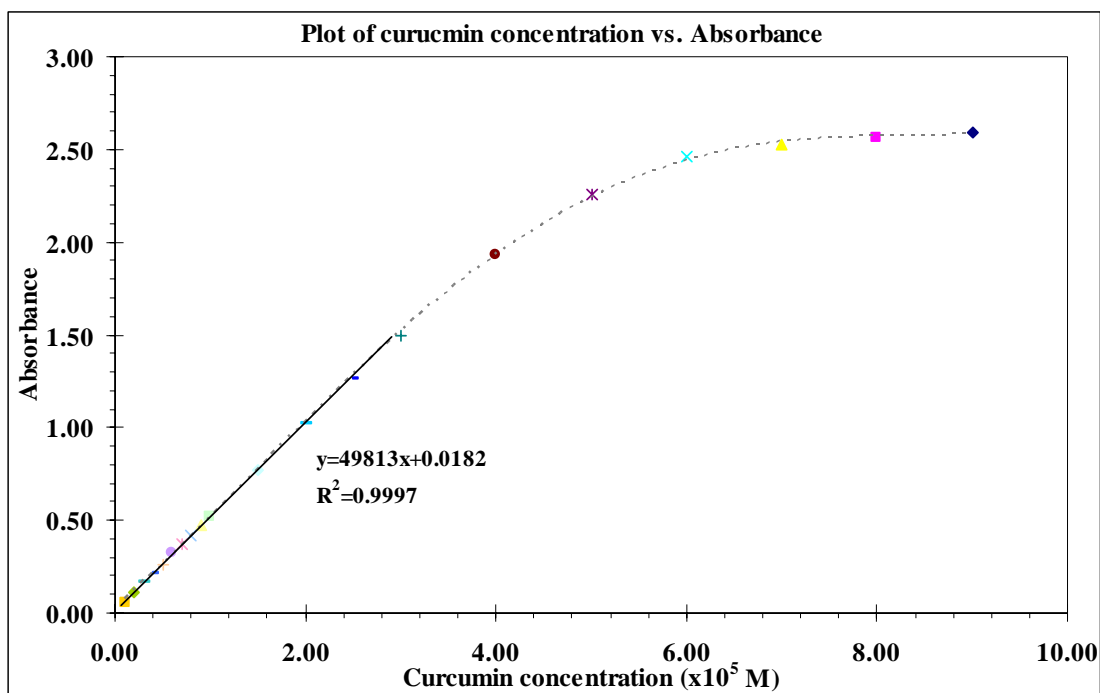


Figure 18 UV-Vis spectra of curcumin at various concentrations



**Figure 19** Plot of curcumin concentrations versus its measured absorbances

The linear range of this plot (at less than  $3.0 \times 10^{-5}$  M) gives the range of suitable concentrations of curcumin to be used in 50% MeOH at 25°C. The deviations of absorbance from the straight line region at concentration  $> 3.0 \times 10^{-5}$  M could be due to self-absorption or insufficient light passing through the cell (Hardy, 2000) or limit of its solubility in 50% MeOH solvent.

### 3.1.2 Effect of some metal ions on curcumin spectra

Curcumin in methanolic media shows a UV-Vis characteristic band around 300-500 nm,  $\lambda_{\max} = 428$  nm, whose intensity decreases on decreasing curcumin concentration. After addition of metal ions that can interact with curcumin, this absorption band may decrease or show some changes in absorbance. In this work, solutions of Ag(I), Cd(II), Cr(III), Cu(II), Fe(II), Fe(III), Hg(II), La(III), Mn(II), Ni(II), Pb(II), and Zn(II) were added to curcumin at various concentrations, and the changes in UV-Vis absorption spectra were recorded as shown in Figures 20 - 33.

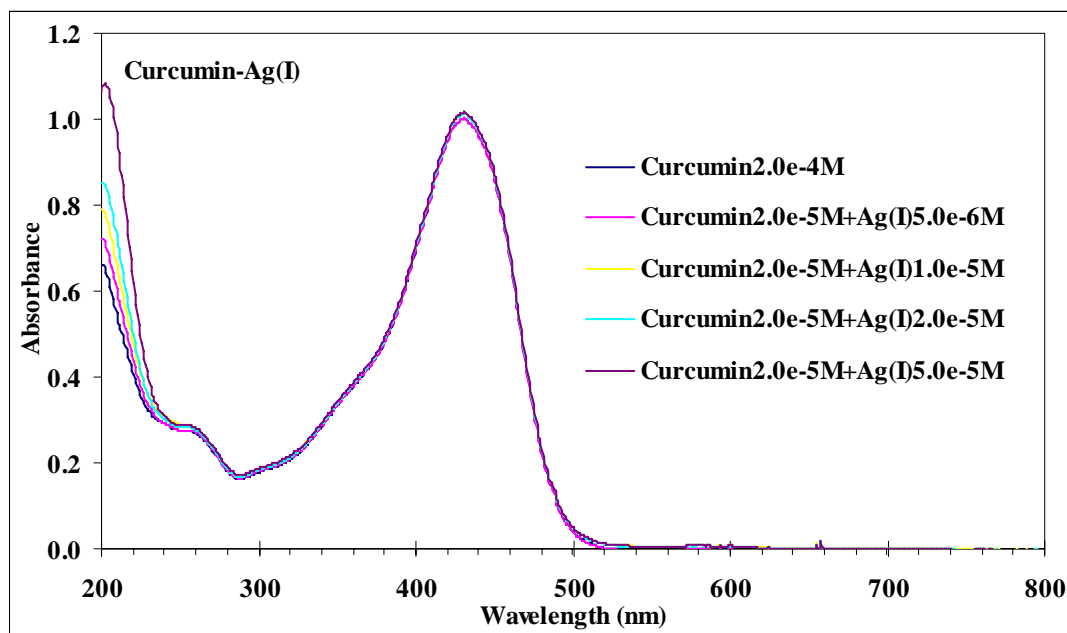


**Figure 20** The UV-Vis spectra of curcumin and curcumin with added Ag(I) ion at various concentrations

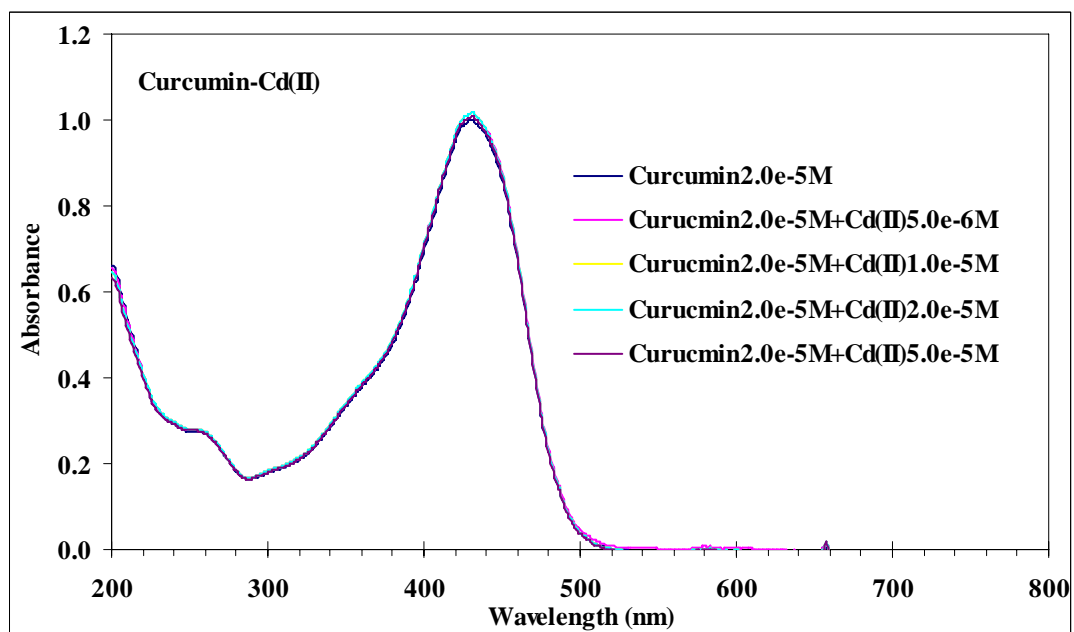


**Figure 21** The UV-Vis spectra of curcumin and curcumin with added Cd(II) ion at various concentrations

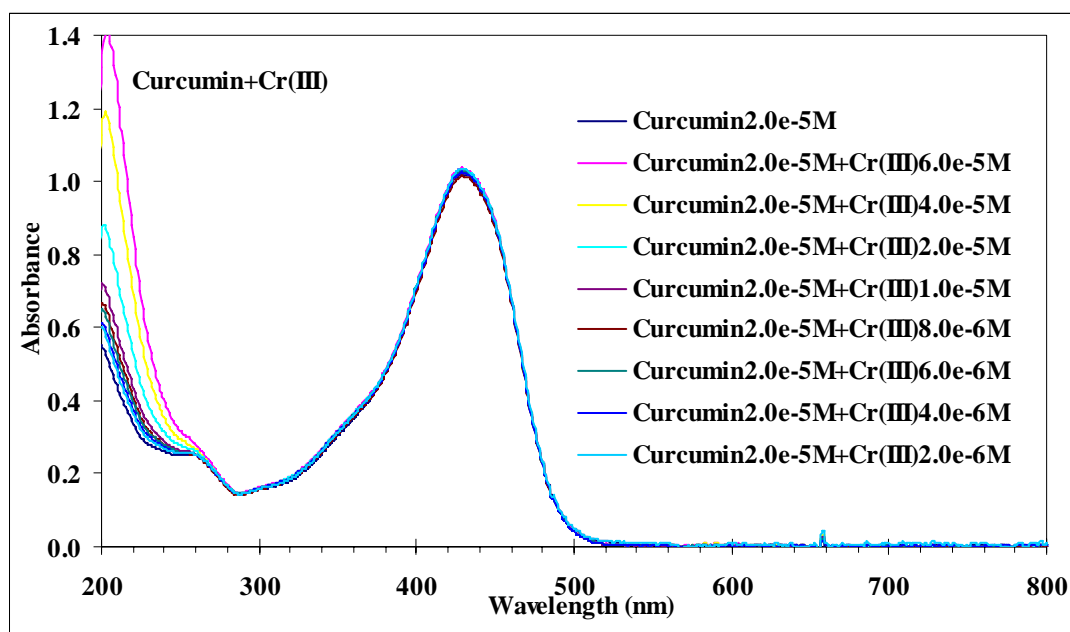


**Figure 22** The UV-Vis spectra of curcumin and curcumin with added Cr(III) ion at various concentrations

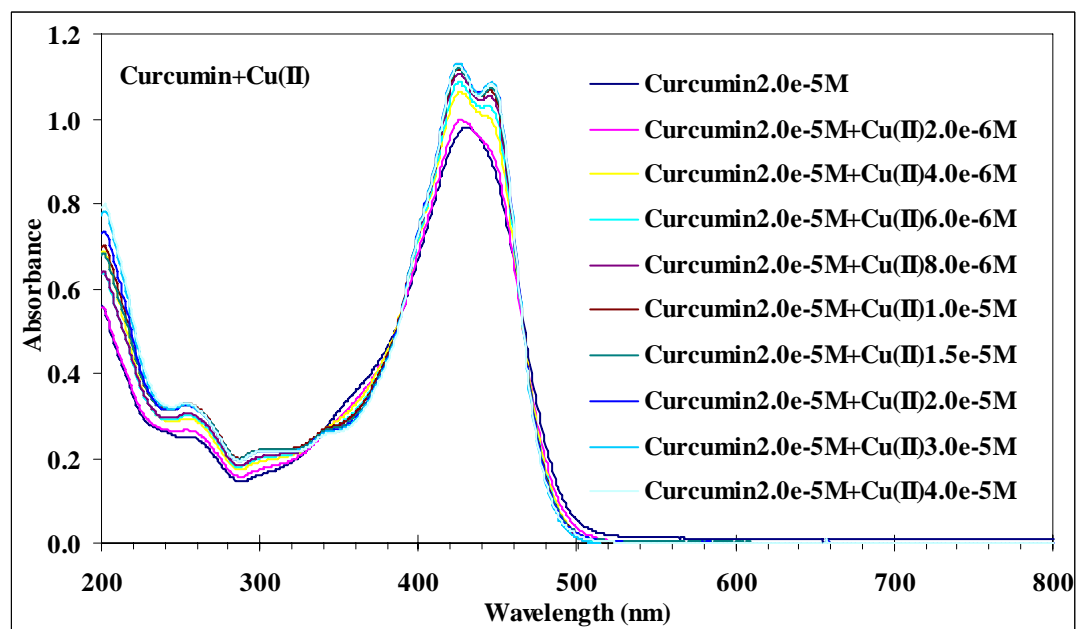


**Figure 23** The UV-Vis spectra of curcumin and curcumin with added Cu(II) ion at various concentrations

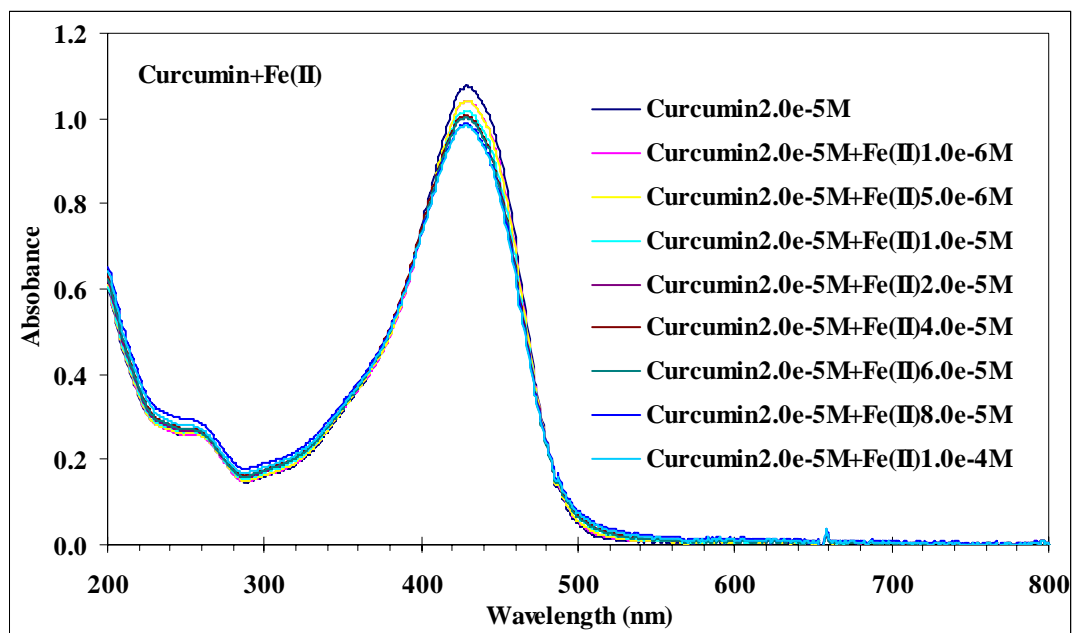


**Figure 24** The UV-Vis spectra of curcumin and curcumin with added Fe(II) ion at various concentrations

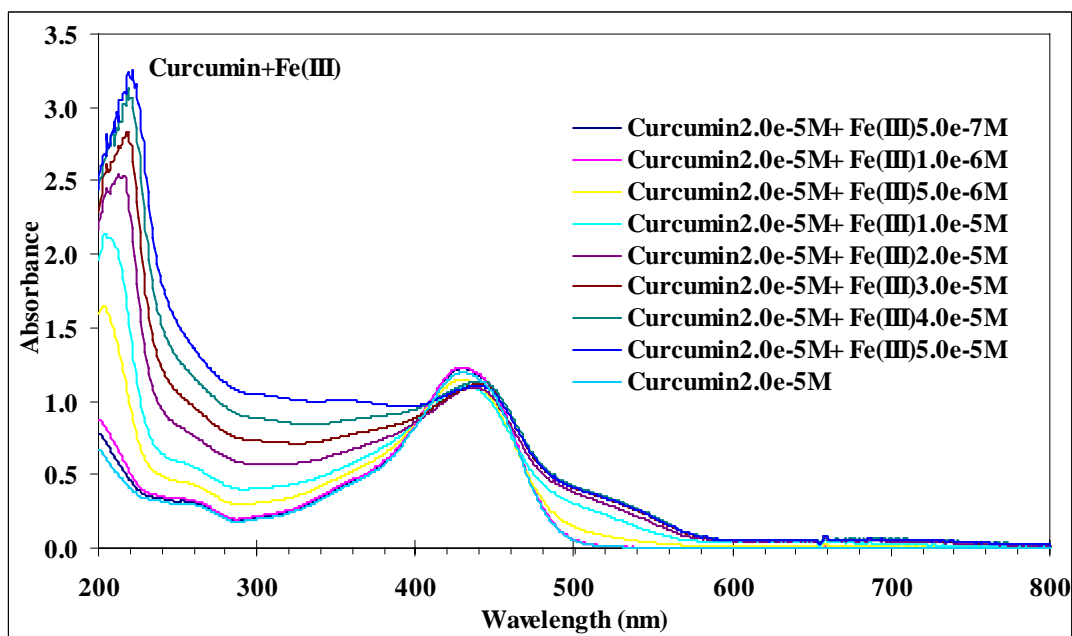


**Figure 25** The UV-Vis spectra of curcumin and curcumin with added Fe(III) ion at various concentrations

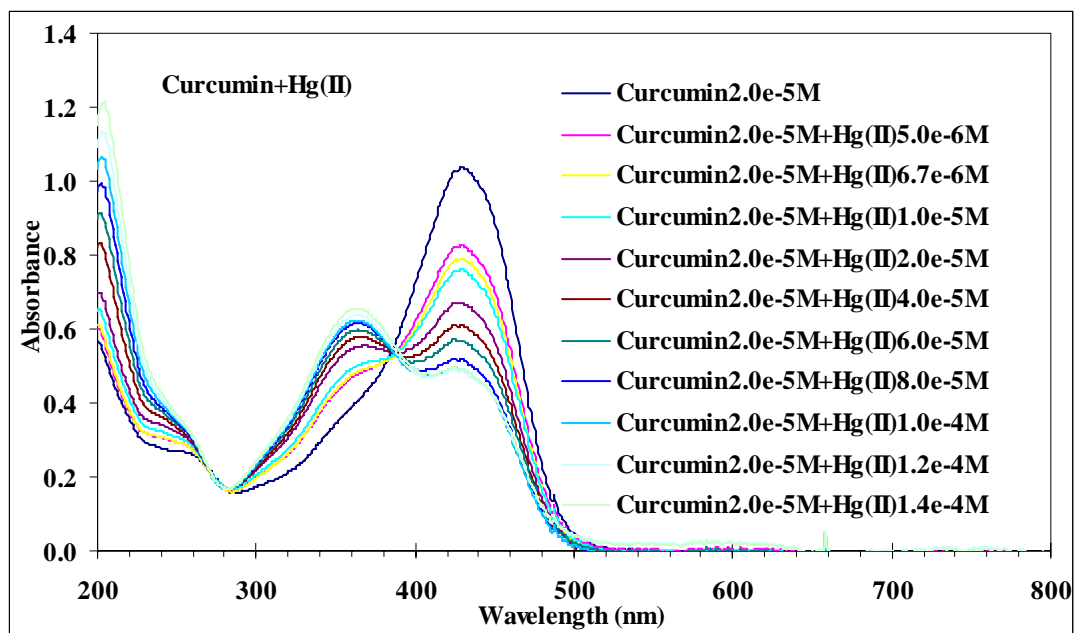


**Figure 26** The UV-Vis spectra of curcumin and curcumin with added Hg(II) ion at various concentrations

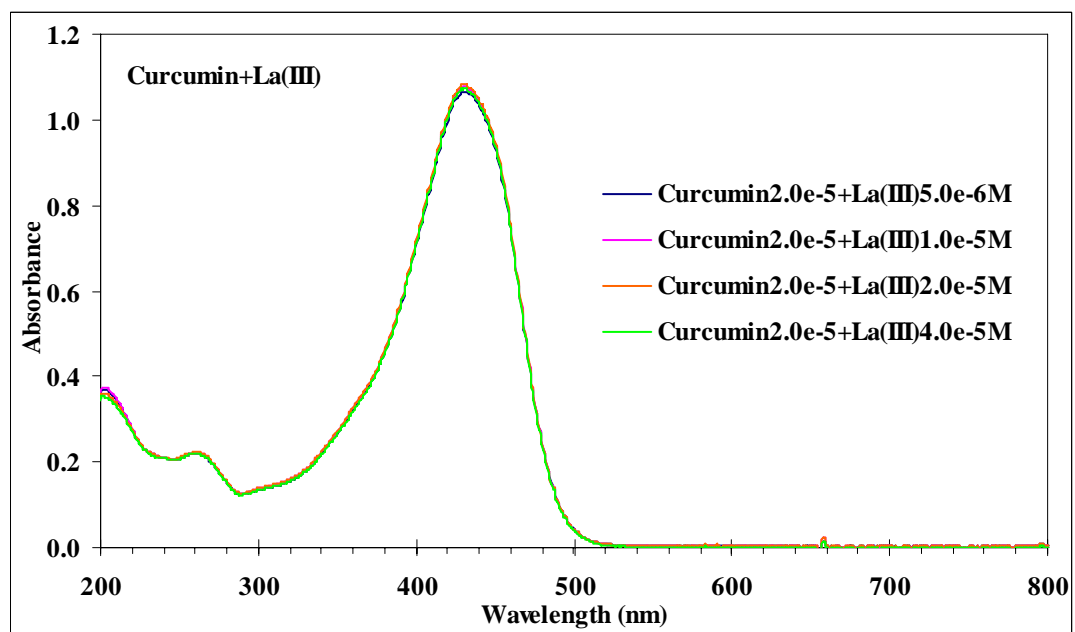


**Figure 27** The UV-Vis spectra of curcumin and curcumin with added La(III) ion ( $\text{La}(\text{CH}_3\text{COO})_3$ ) at various concentrations

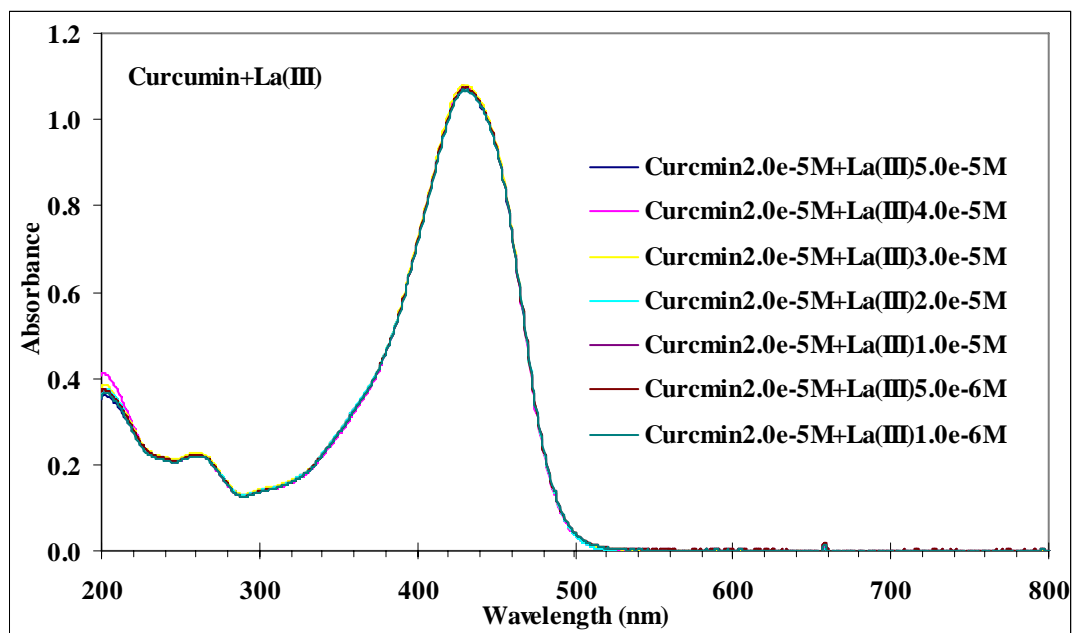


**Figure 28** The UV-Vis spectra of curcumin and curcumin with added La(III) ion ( $\text{LaCl}_3$ ) at various concentrations

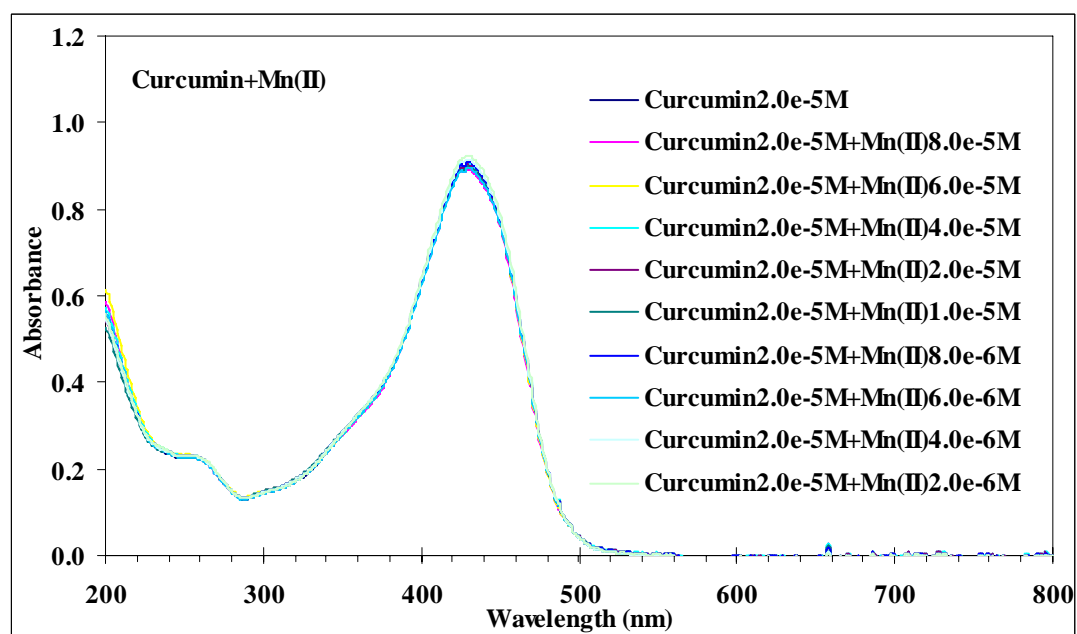


**Figure 29** The UV-Vis spectra of curcumin and curcumin with added Mn(II) ion at various concentrations

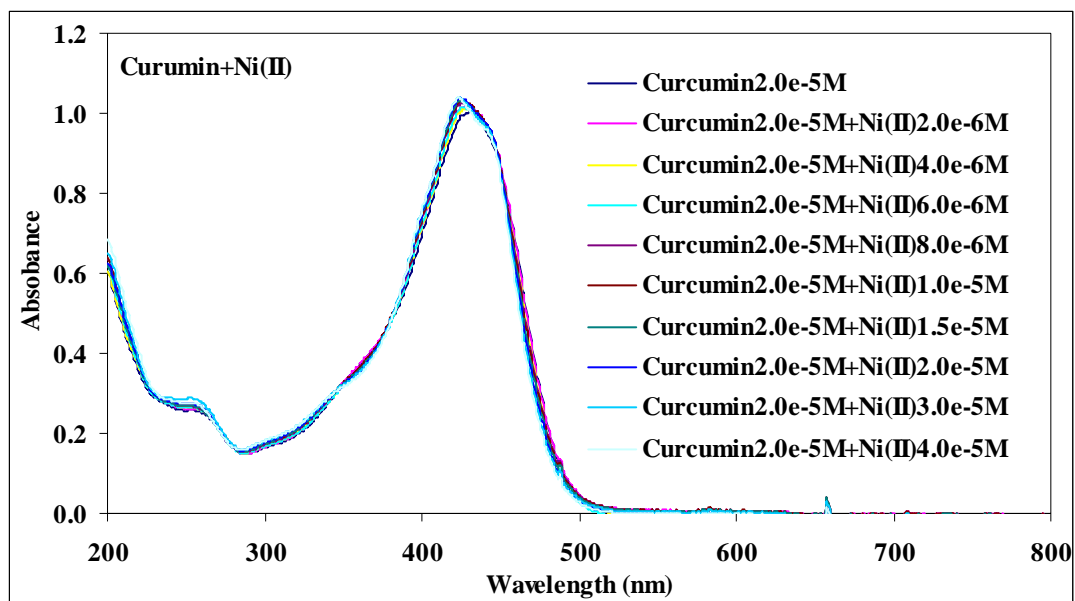


**Figure 30** The UV-Vis spectra of curcumin and curcumin with added Ni(II) ion ( $\text{NiCl}_2$ ) at various concentrations

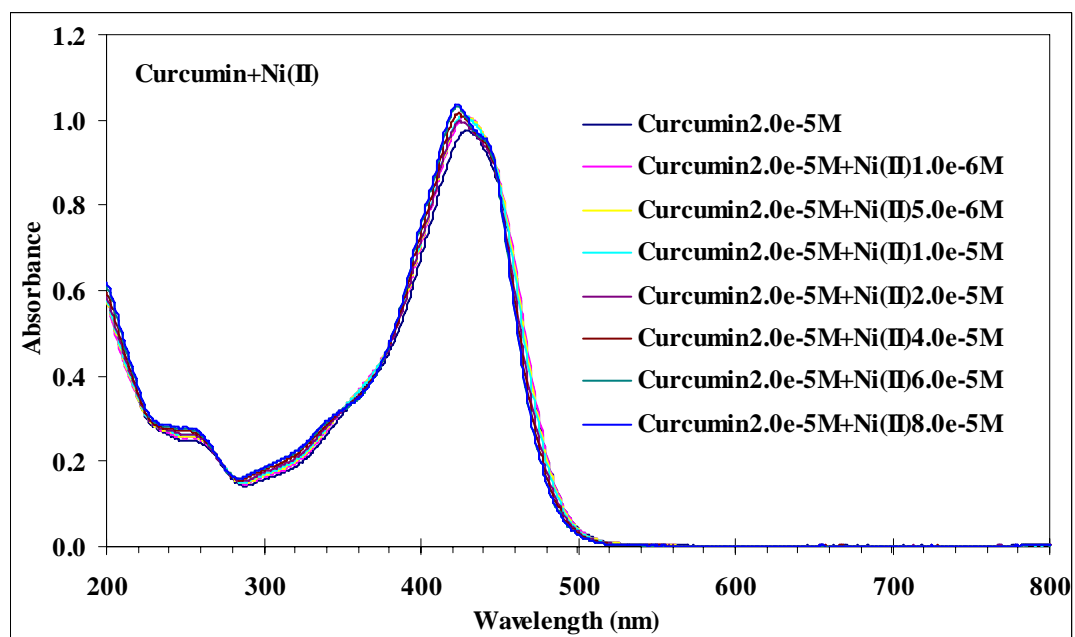


**Figure 31** The UV-Vis spectra of curcumin and curcumin with added Ni(II) ion ( $\text{Ni}(\text{SO}_4)_2$ ) at various concentrations



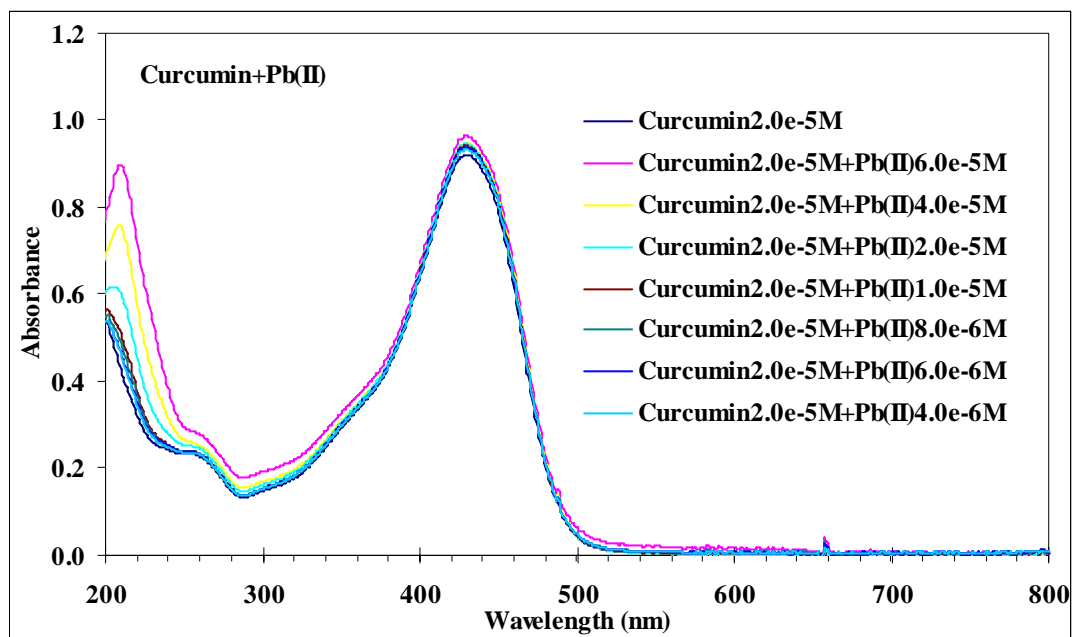


**Figure 32** The UV-Vis spectra of curcumin and curcumin with added Pb(II) ion at various concentrations

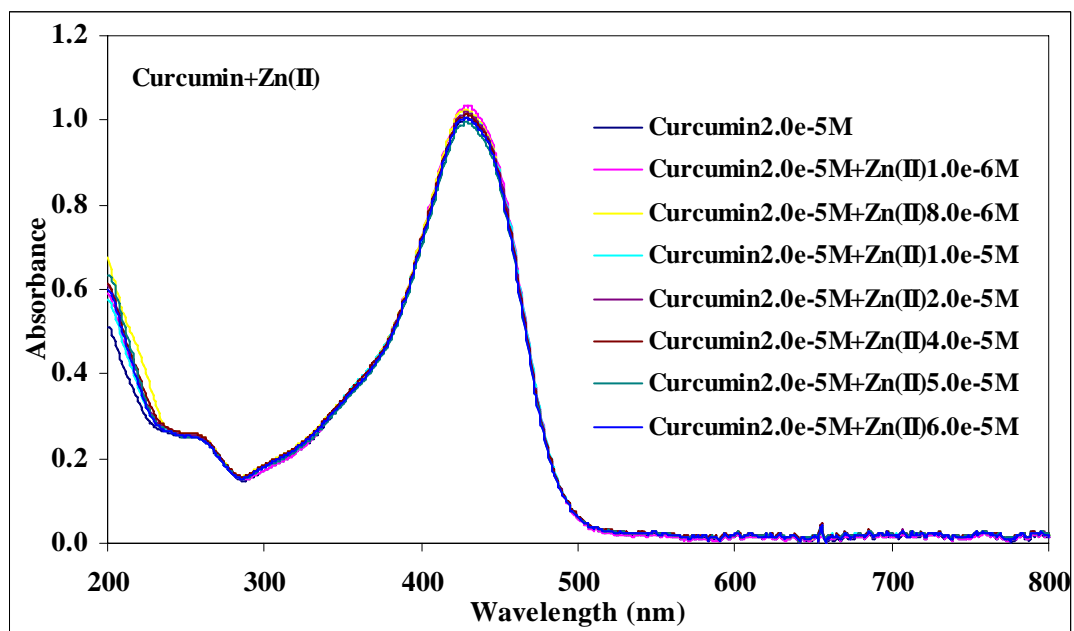


**Figure 33** The UV-Vis spectra of curcumin and curcumin with added Zn(II) ion at various concentrations

Among all the metal ions added only Cu(II), Fe(II), Fe(III), Hg(II), and Ni(II) caused some changes in curcumin absorption. The addition of Cu(II) caused the absorption band of curcumin at 430 nm splitting into 425 and 445 nm with increase in intensity. In the case of Fe(II) the intensity of the absorption band decreased while addition of Fe(III) also caused the absorption intensity at 430 nm to decrease with bathochromic shift to 445 nm due to a new weak absorption band at 510 nm. When Hg(II) was added a decrease in intensity at the maximum absorption was observed with a new absorption band appeared at wavelength 368 nm giving an isosbestic point at 390 nm. Addition of Ni(II) caused the maximum absorption at 430 nm to shift to shorter wavelength (hypsochromic) 423 nm with slight increased in intensity. These observations were signs showing some interactions between metal ions and curcumin.

### **3.1.3 Stability of curcumin-metal spectra with time**

Mixed solutions of curcumin and metal ions were studied with time to see whether any changes would take place. The change in absorption spectra of curcumin-Cu(II), curcumin-Fe(II), curcumin-Fe(III), curcumin-Hg(II), and curcumin-Ni(II) systems are shown in Figures. 34, 36, 38, 40, and 42, respectively, and the plot of their maximum absorption against time are illustrated in Figures. 35, 37, 39, 41, and 43, respectively.

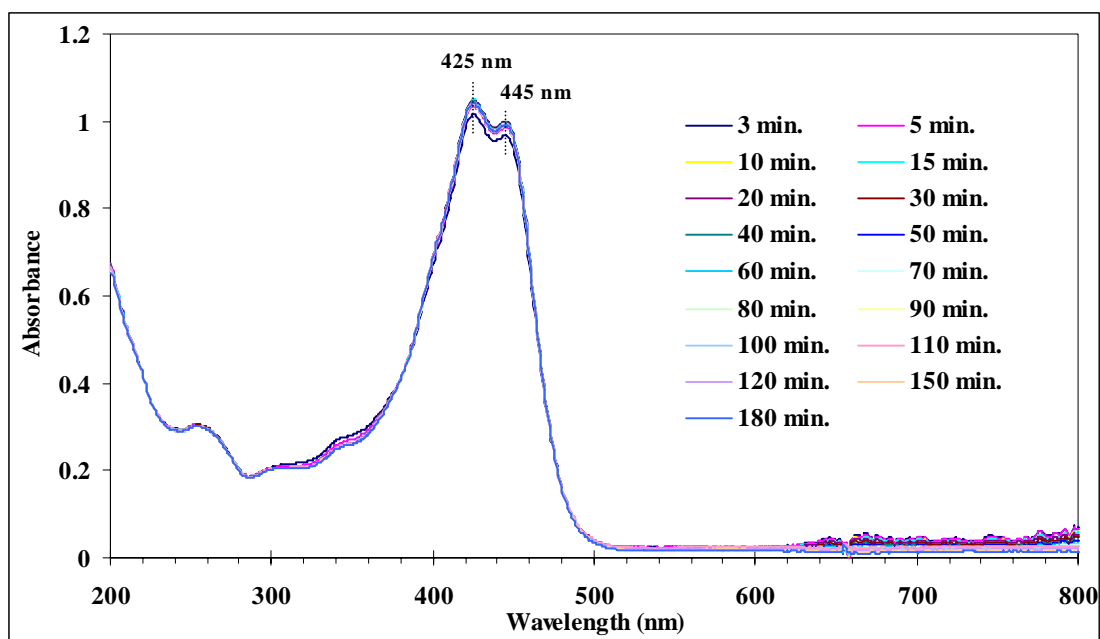


**Figure 34** UV-Vis spectra of curcumin ( $2.0 \times 10^{-5}$  M) after addition of Cu(II) ( $1.0 \times 10^{-5}$  M) at various times in 50% MeOH

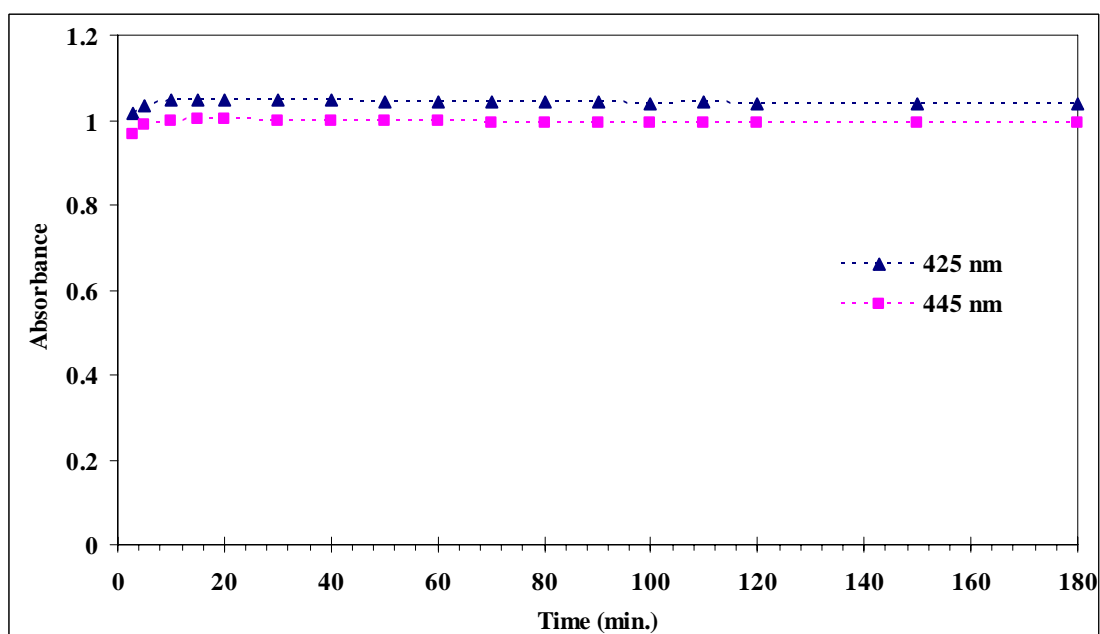


**Figure 35** Plot of time versus maximum absorbance and the shoulder from Figure 34

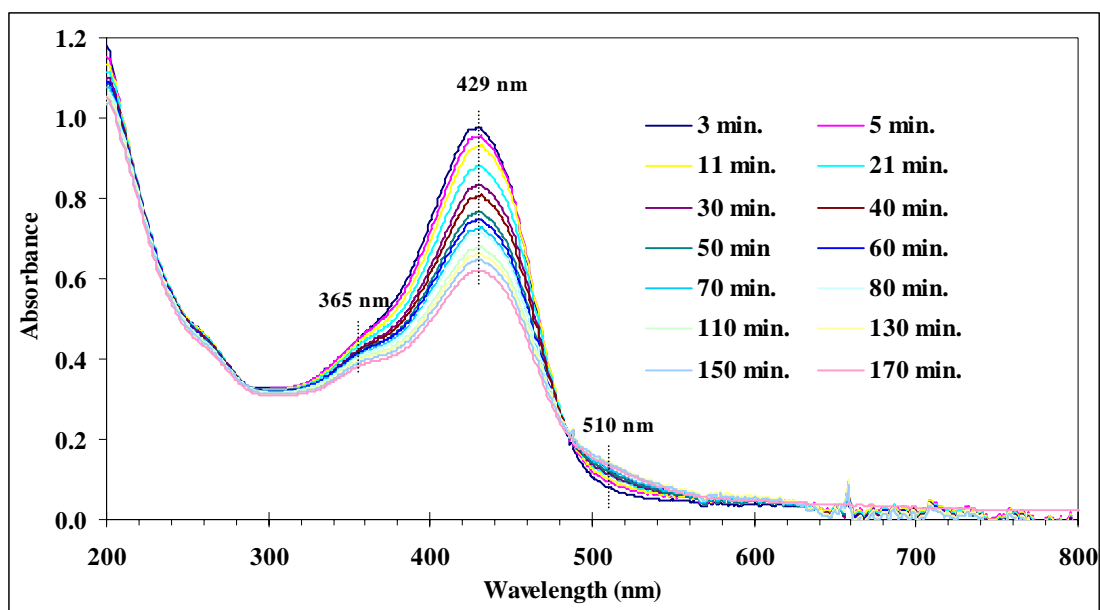


**Figure 36** UV-Vis spectra of curcumin ( $2.0 \times 10^{-5}$  M) after addition of  $\text{Fe(II)}$  ( $2.0 \times 10^{-5}$  M) at various times in 50% MeOH

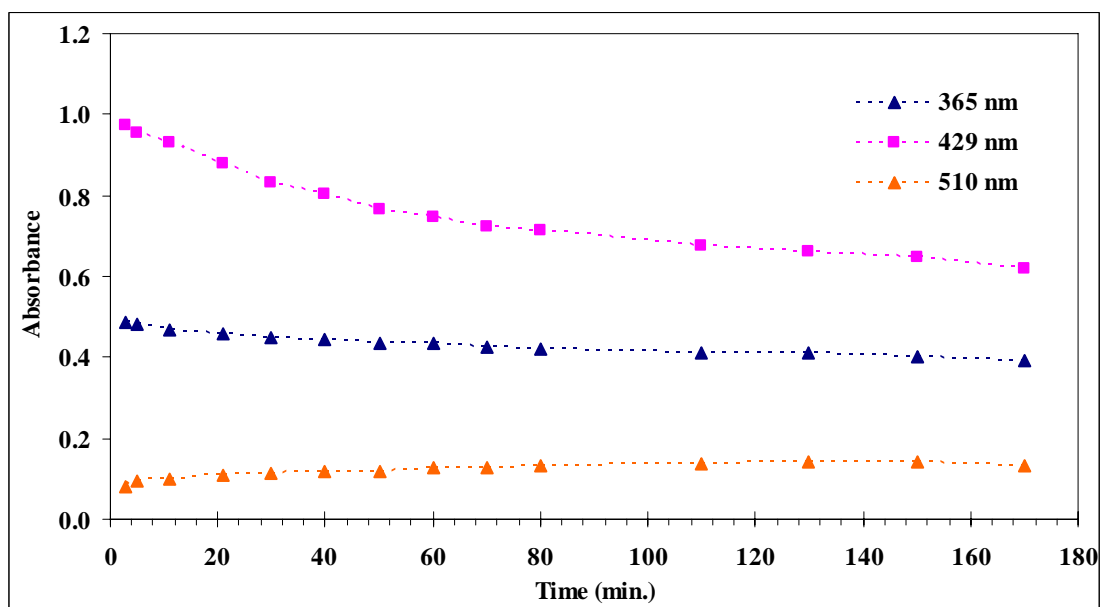


**Figure 37** Plot of time versus maximum absorbance the shoulder, and the new absorption from Figure 36

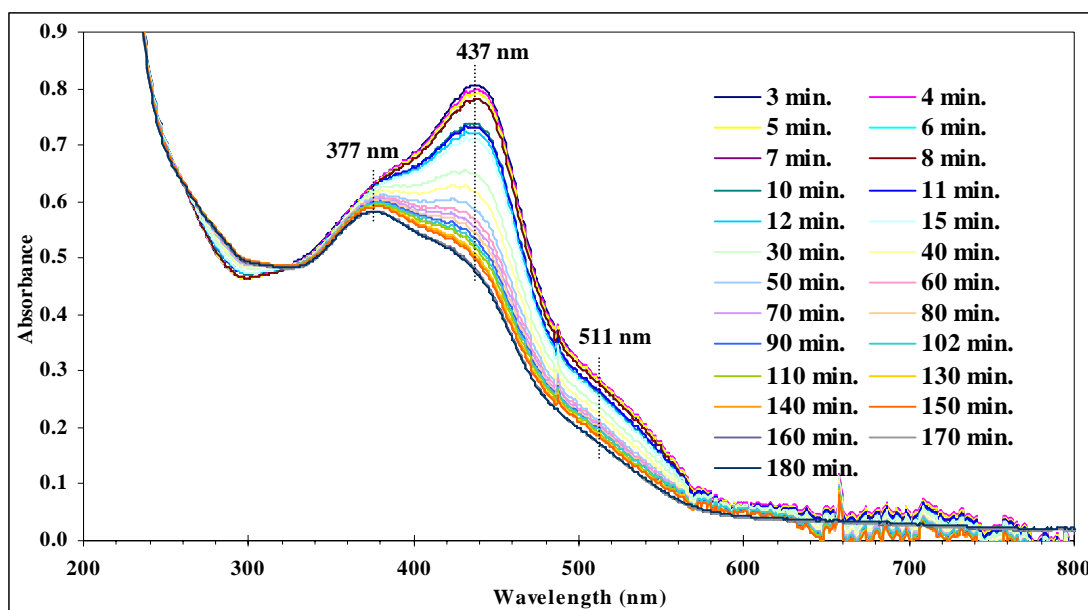


**Figure 38** UV-Vis spectra of curcumin ( $2.0 \times 10^{-5}$  M) after addition of Fe(III) ( $1.0 \times 10^{-5}$  M) at various times in 50% MeOH

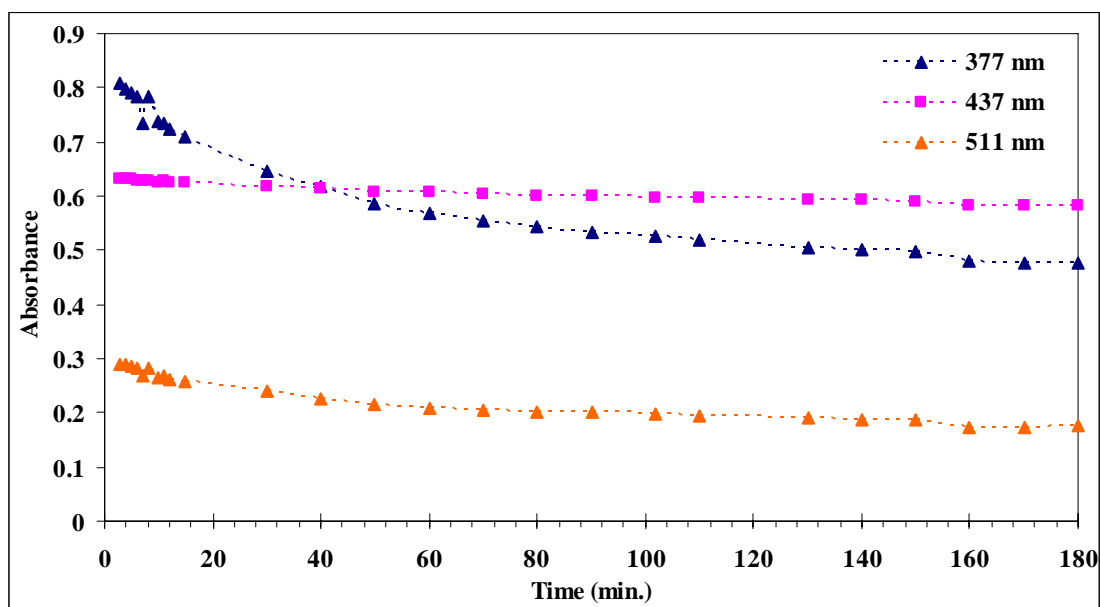


**Figure 39** Plot of time versus maximum absorbance and the shoulders from Figure 38

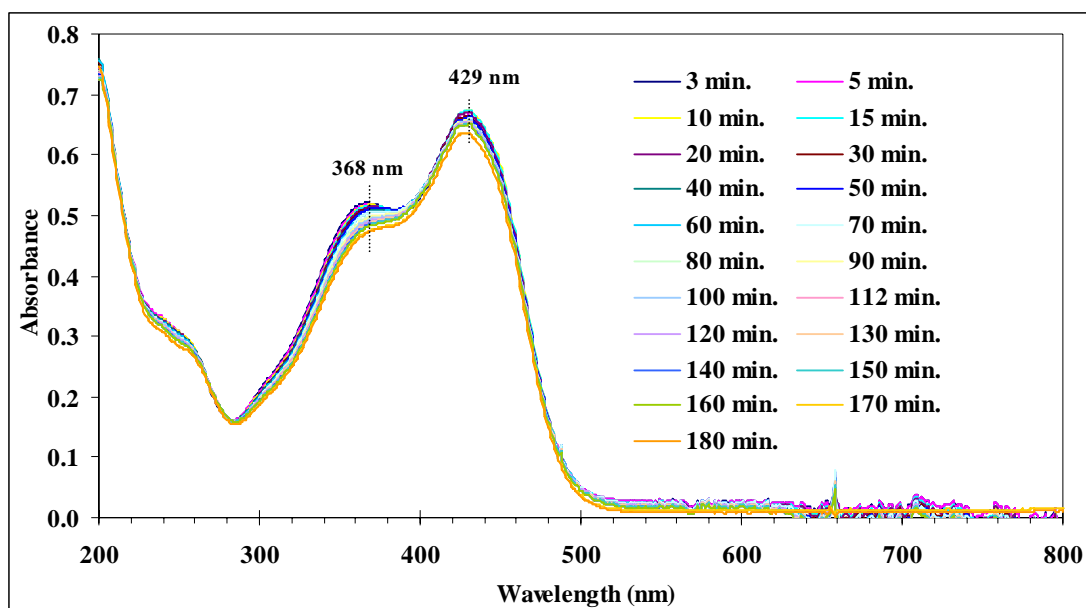


**Figure 40** UV-Vis spectra of curcumin ( $2.0 \times 10^{-5}$  M) after addition of Hg(II) ( $2.0 \times 10^{-5}$  M) at various times in 50% MeOH

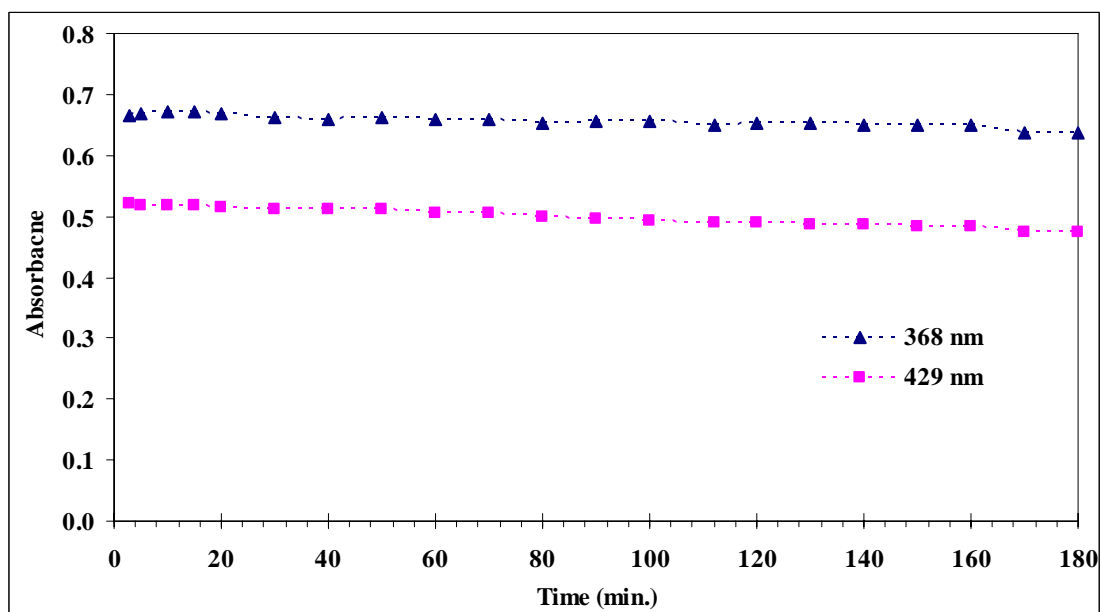


**Figure 41** Plot of time versus maximum absorbance and the shoulder from Figure 40

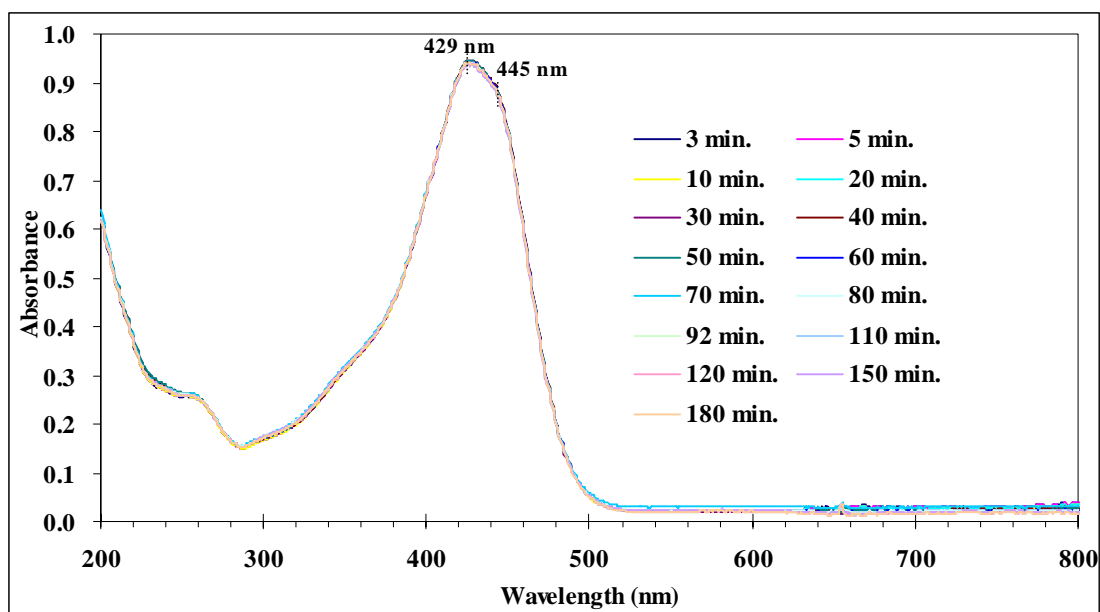


**Figure 42** UV-Vis spectra of curcumin ( $2.0 \times 10^{-5}$  M) after addition of  $\text{Ni(II)}$  ( $1.0 \times 10^{-5}$  M) at various times in 50% MeOH

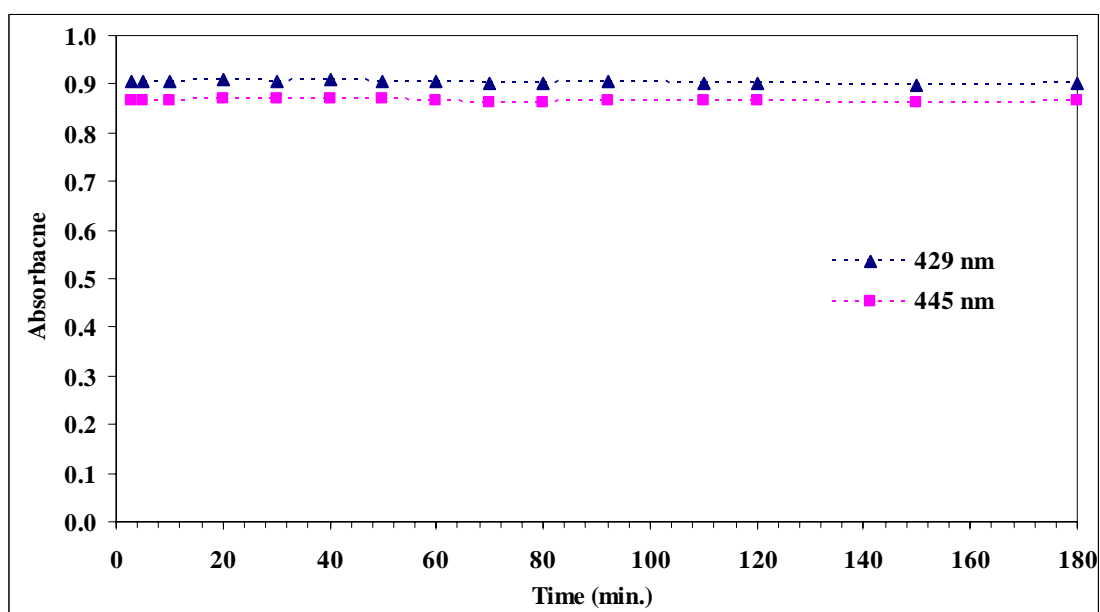


**Figure 43** Plot of time versus maximum absorbance and the shoulder from Figure 42

In the spectra acquisition, the concentrations of both curcumin and metal ion were fixed, the solutions were protected from light and the temperature was kept constant. Over the 3 hours period, the absorption intensities of curcumin-Cu(II), curcumin-Hg(II), and curcumin-Ni(II) systems were constant, but the curcumin-Fe(II) and curcumin-Fe(III) systems showed a large decrease of curcumin absorption band (430 nm) which may be due to some interaction between curcumin and Fe(II) or Fe(III) ions. Fe(III) tends to be reduced to Fe(II) over time which can be observed by the increase in absorbance at 510 nm. Curcumin has been reported as a Fe(III) reducing agent by Tønnessen and Greenhill (Tønnessen and Greenhill, 1992).

Those metal ions that caused changes in the spectrum of curcumin, i.e. indicating some interaction with curcumin, were Cu(II) ( $\text{CuCl}_2 \cdot 2\text{H}_2\text{O}$ ), Fe(II) ( $\text{FeSO}_4 \cdot 7\text{H}_2\text{O}$ ), Fe(III) ( $\text{Fe}(\text{NO}_3)_3 \cdot 9\text{H}_2\text{O}$ ), Hg(II) ( $\text{HgCl}_2$ ), Ni(II) ( $\text{NiCl}_2 \cdot 6\text{H}_2\text{O}$ ), and ( $\text{NiSO}_4 \cdot 6\text{H}_2\text{O}$ ). Of these, Cu(II), Ni(II), and Hg(II) were chosen for further studies. Fe(II) and Fe(III) were excluded due to their complicated nature in the reactions that were observed in this work. Both Fe ions have been studied and reported but their behaviors which we observed in this work were not mentioned in those reports (Tønnessen and Greenhill, 1992; Bernabé-Pineda, *et al.*, 2004).

## **3.2 Study on the stoichiometry of curcumin-metal ion complexes**

### **3.2.1 Study on the stoichiometry of curcumin-Cu(II), curcumin-Hg(II), curcumin-Ni(II) complexes by the mole-ratio method**

The stoichiometry of these complexes were studied by using the mole-ratio method. The change in absorption spectra of curcumin-Cu(II), curcumin-Hg(II), and curcumin-Ni(II) systems are shown in Figures 44, 46, and 48, respectively, and their mole-ratio plot are shown in Figures 45, 47, and 49, respectively.



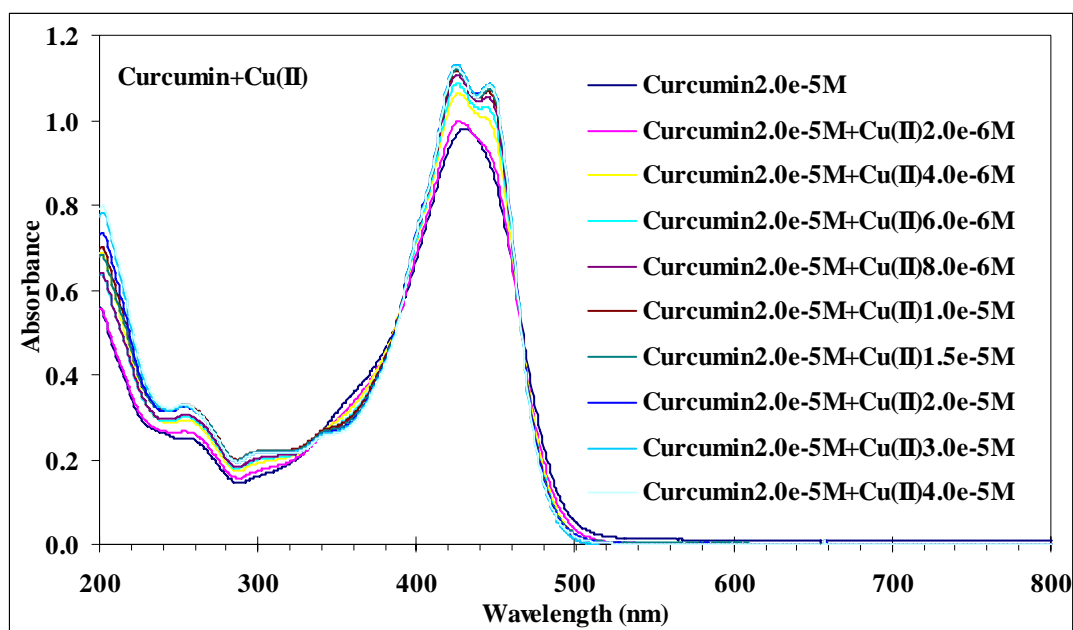


**Figure 44** Changes of curcumin spectra when added Cu(II) at various concentrations

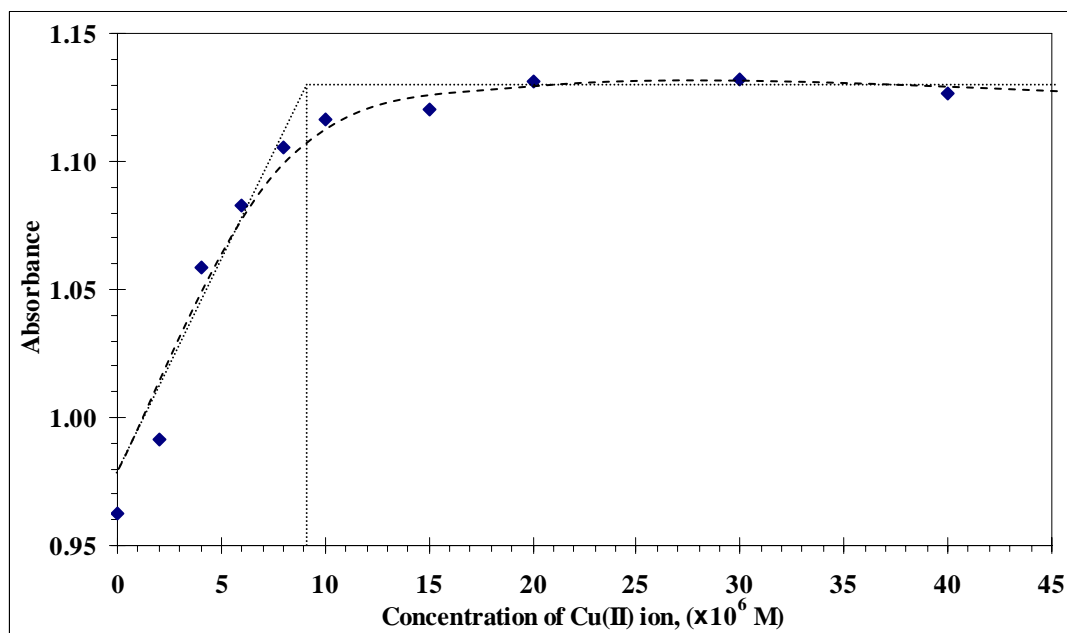


**Figure 45** The mole-ratio plot of absorbance versus the added concentration of Cu(II) ion from Figure 44

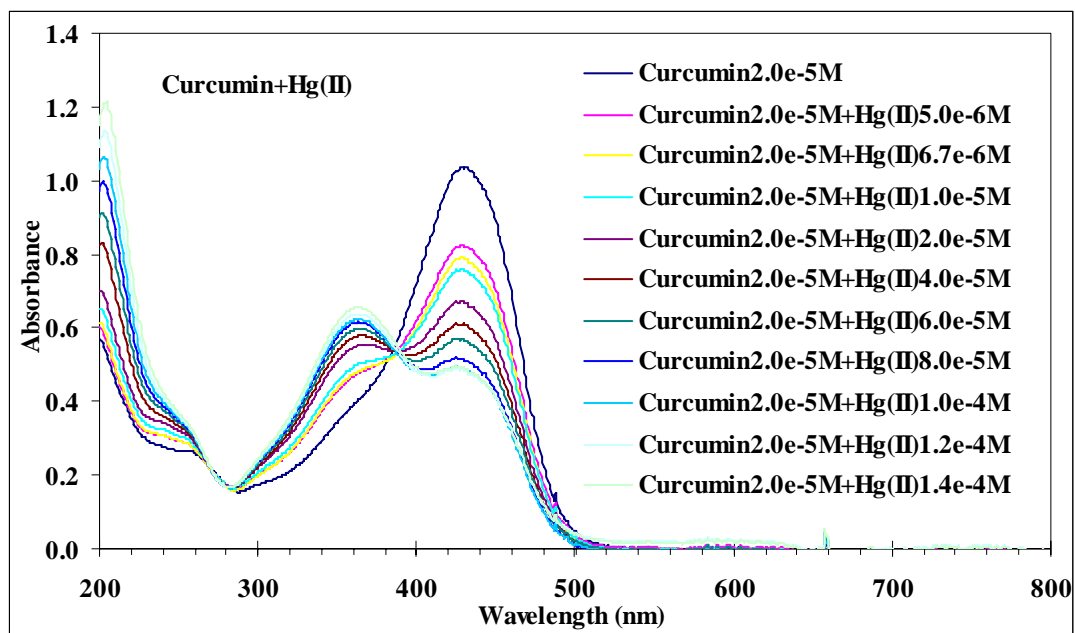


Figure 46 Changes of curcumin spectra when added Hg(II) at various concentrations

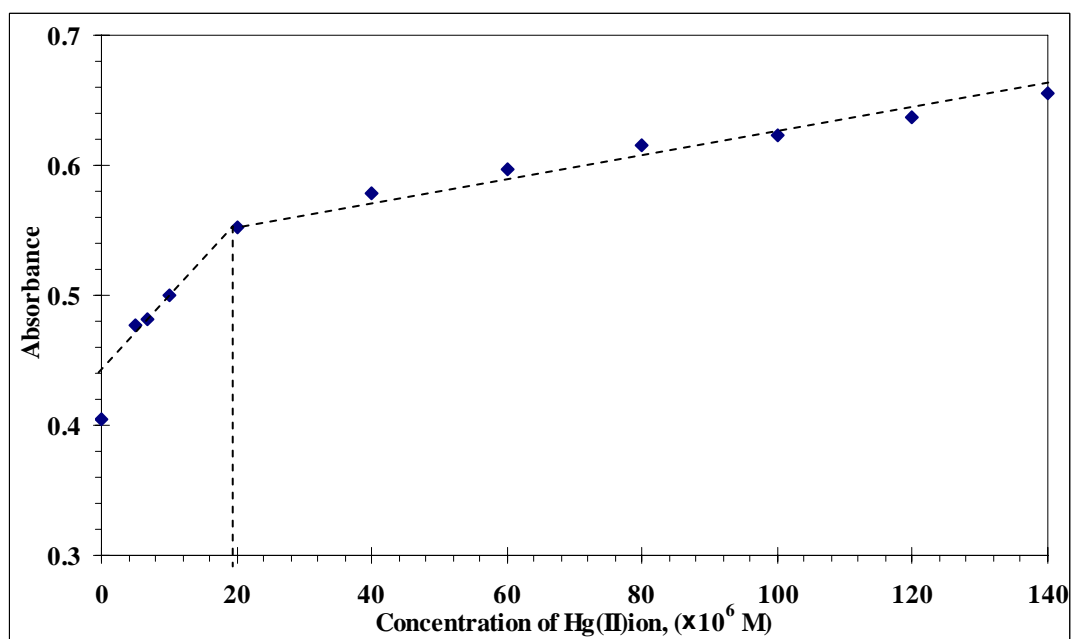
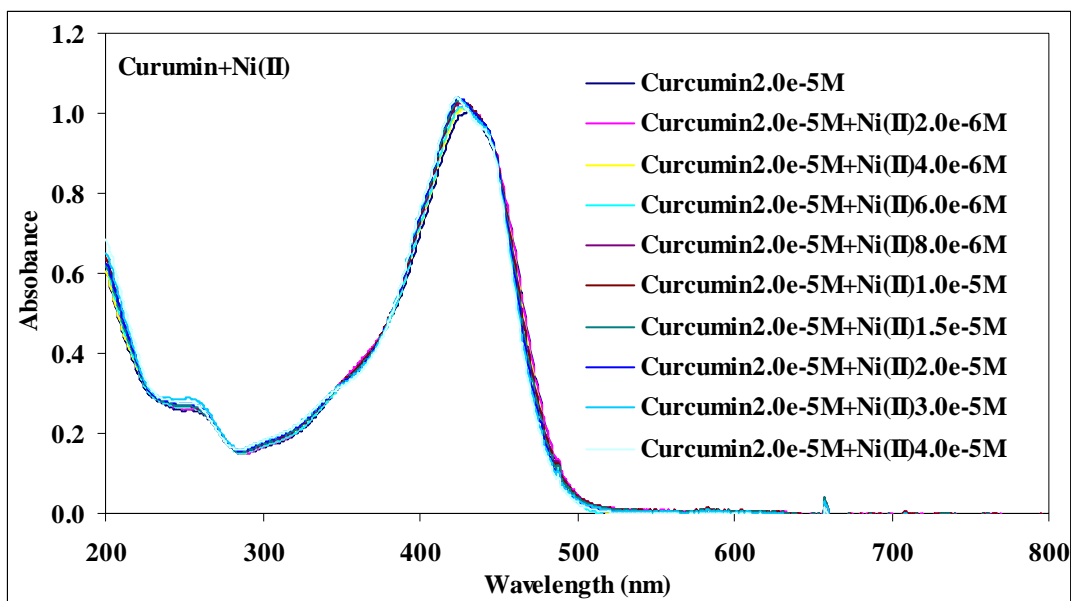
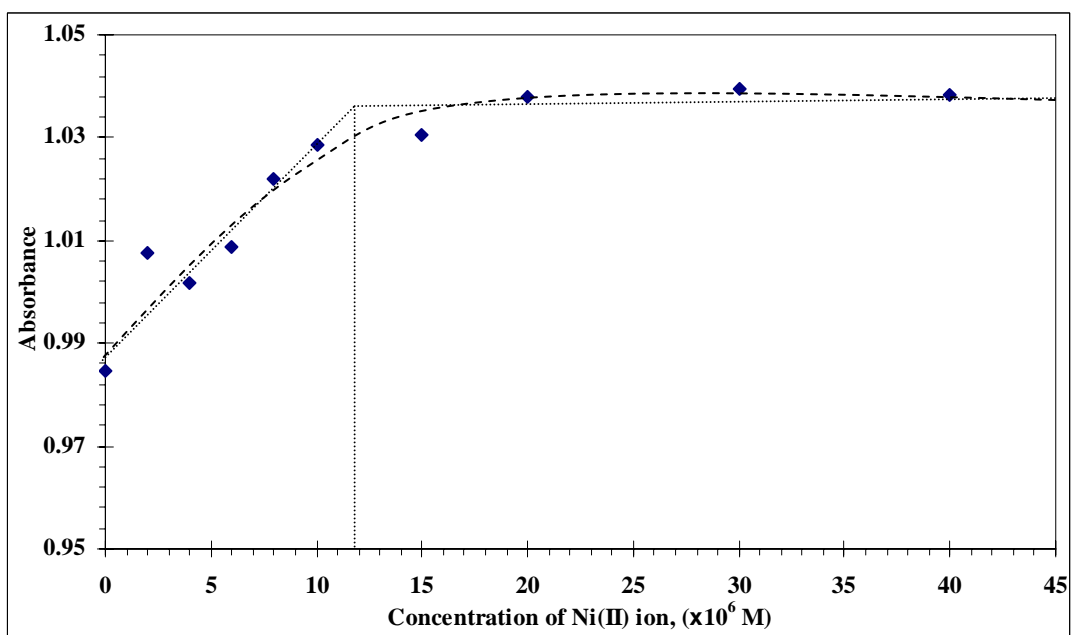


Figure 47 The mole-ratio plot of absorbance versus the added concentration of Hg(II) ion from Figure 46



**Figure 48** Changes of curcumin spectra when added Ni(II) at various concentrations



**Figure 49** The mole-ratio plot of absorbance versus the added concentration of Ni(II) ion from Figure 48

Mole-ratio plot of these curcumin-metal systems show an inflection curve, which the concentration of metal ion that in equilibrium with curcumin ( $2.0 \times 10^{-5}$

M) can be read off from the intersection point. The stoichiometric ratio of curcumin to Cu(II) ( $2.0 \times 10^{-5} : 9.3 \times 10^{-6}$ ), and Ni(II) ( $2.0 \times 10^{-5} : 1.2 \times 10^{-5}$ ) are 2:1 and curcumin to Hg(II) is 1:1 ( $2.0 \times 10^{-5} : 1.9 \times 10^{-5}$ ).

### 3.2.2 Study on the stoichiometry of curcumin-Cu(II), curcumin-Hg(II), curcumin-Ni(II) complexes by the mole-ratio method after subtraction of the residual free curcumin absorption

The spectrophotometric data of curcumin-Cu, curcumin-Hg(II), and curcumin-Ni(II) in 3.2.1 were numerically subtracted to remove the unreacted curcumin and shown in Figures. 50, 52, and 54, respectively. Moreover, their mole-ratio plots of them are illustrated in Figures. 51, 53, and 55 respectively.

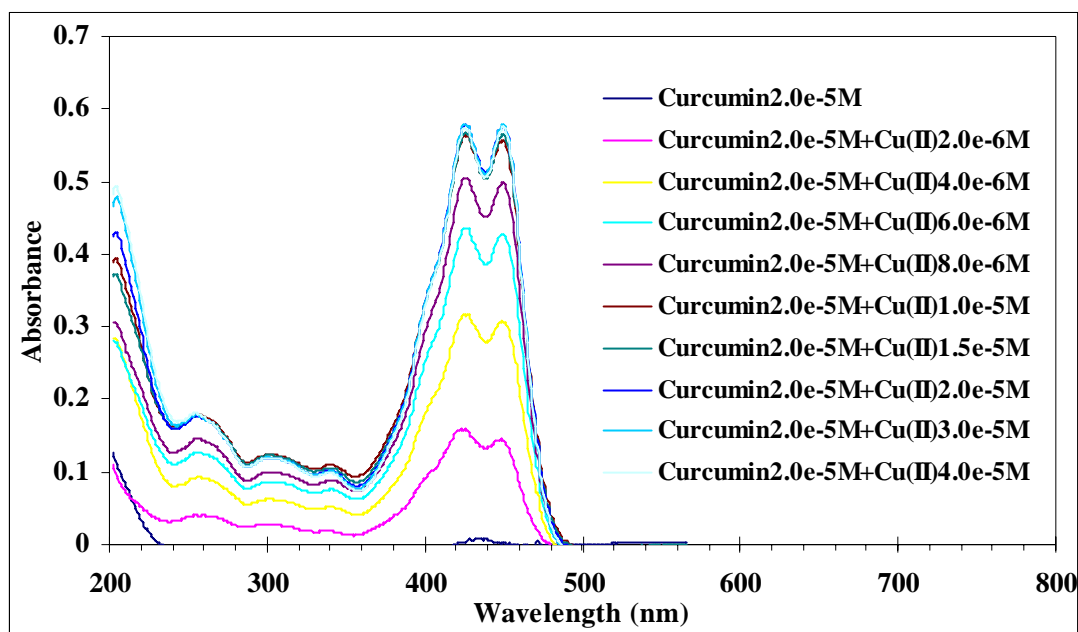


**Figure 50** UV-Vis spectra of curcumin-Cu(II) complex (after subtracted the residual free curcumin from Figure 39)

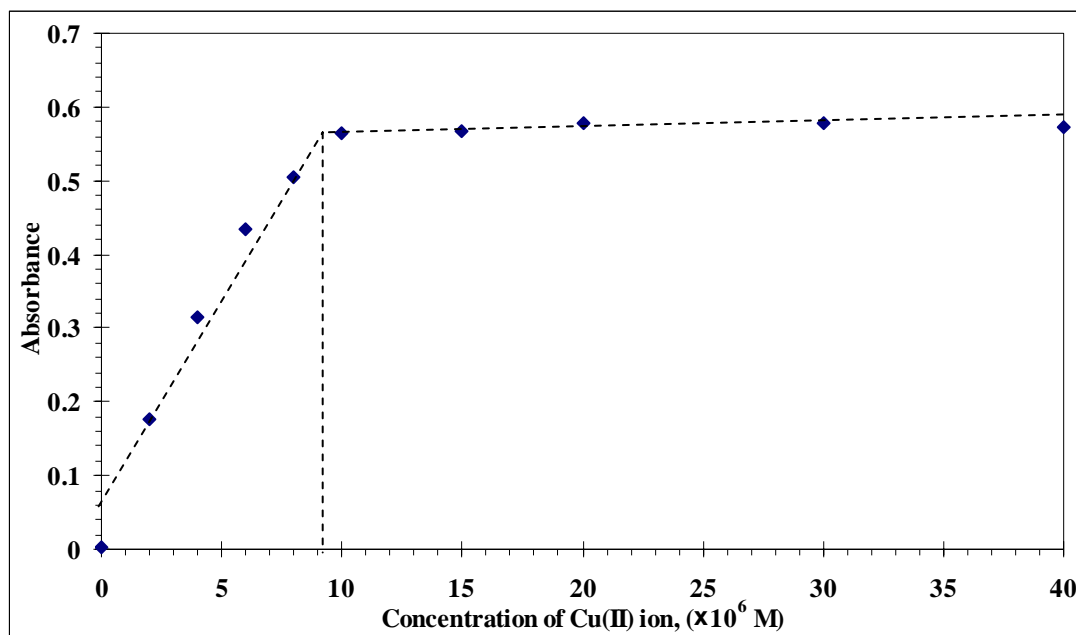


**Figure 51** Mole-ratio plot of curcumin-Cu(II) complex (after subtracted the residual free curcumin from Figure 50, see Figure 45 for comparison)

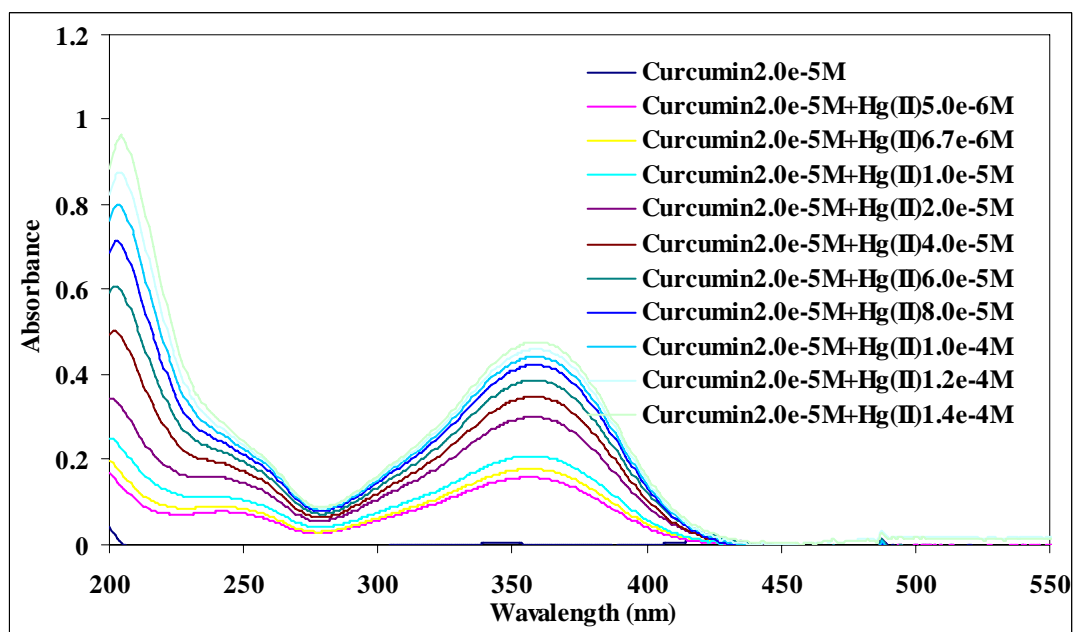


**Figure 52** UV-Vis spectra of curcumin-Hg(II) complex (after subtracted the residual free curcumin from Figure 46)

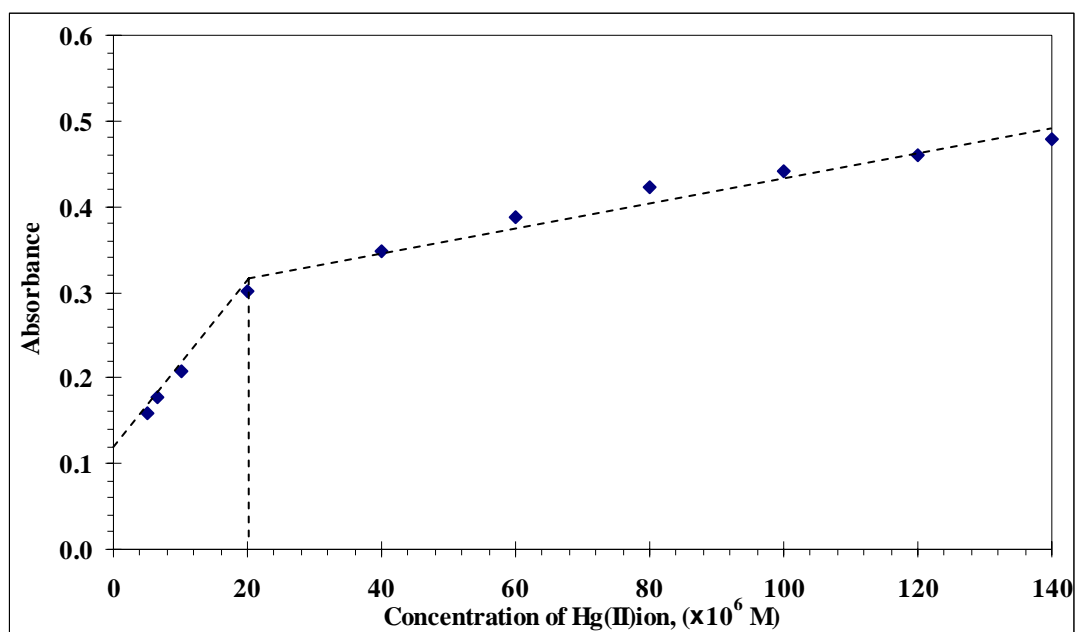


**Figure 53** Mole-ratio plot of curcumin-Hg(II) complex (after subtracted the residual free curcumin from Figure 52, see Figure 47 for comparison)

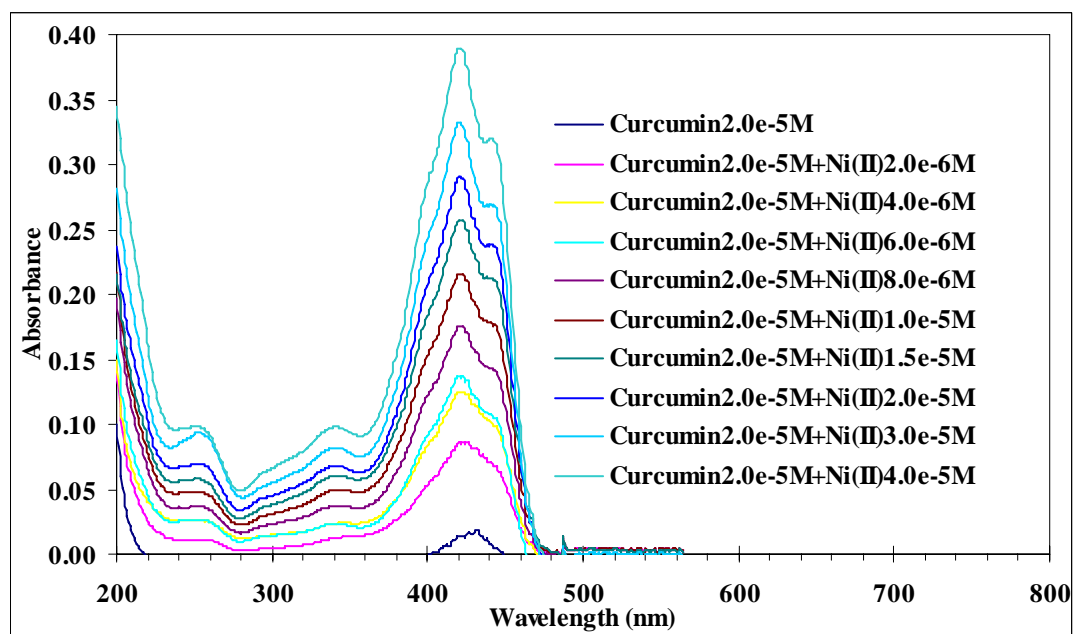


**Figure 54** UV-Vis spectra of curcumin-Ni(II) complex (after subtracted the residual free curcumin from Figure 48)

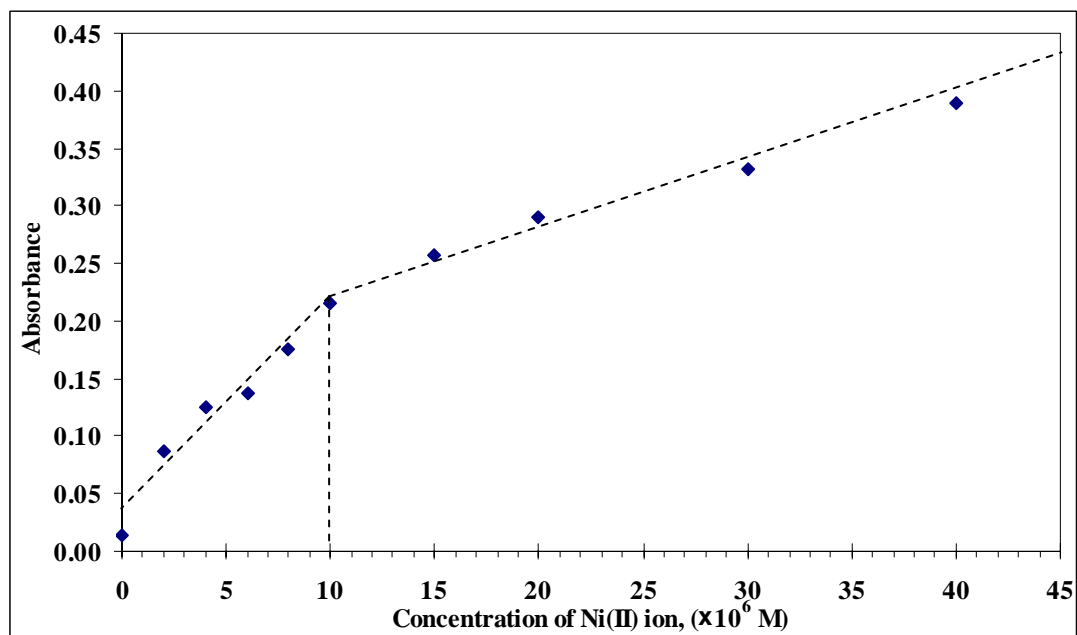


**Figure 55** Mole-ratio plot of curcumin-Ni(II) complex (after subtracted the residual free curcumin from Figure 54, see Figure 49 for comparison)

After subtracted the residual free curcumin, the mole-ratio plot of these curcumin-metal complexes gave a clear interception of two linear parts. The ratio of total concentrations of metal to ligand curcumin ( $2.0 \times 10^{-5}$  M) at the intersection gives the metal ion to curcumin ratio in the complex. The stoichiometric ratios of curcumin to Cu(II), Hg(II), and Ni(II) obtained by this method were  $2.0 \times 10^{-5} : 9.3 \times 10^{-6}$  (2:1),  $2.0 \times 10^{-5} : 2.0 \times 10^{-5}$  (1:1), and  $2.0 \times 10^{-5} : 1.0 \times 10^{-5}$  (2:1), respectively.

### 3.2.3 Study on the stoichiometry of curcumin-Cu(II), curcumin-Hg(II), curcumin-Ni(II) complexes by the continuous variation method

The stoichiometry of these complexes were also studied by continuous variation method (Job's method). The change in absorption spectra of curcumin-Cu(II), curcumin-Hg(II), and curcumin-Ni(II) systems are shown in Figures 56, 58, and 60, respectively, and their Job's plots are shown in Figures 57, 59, and 61, respectively.

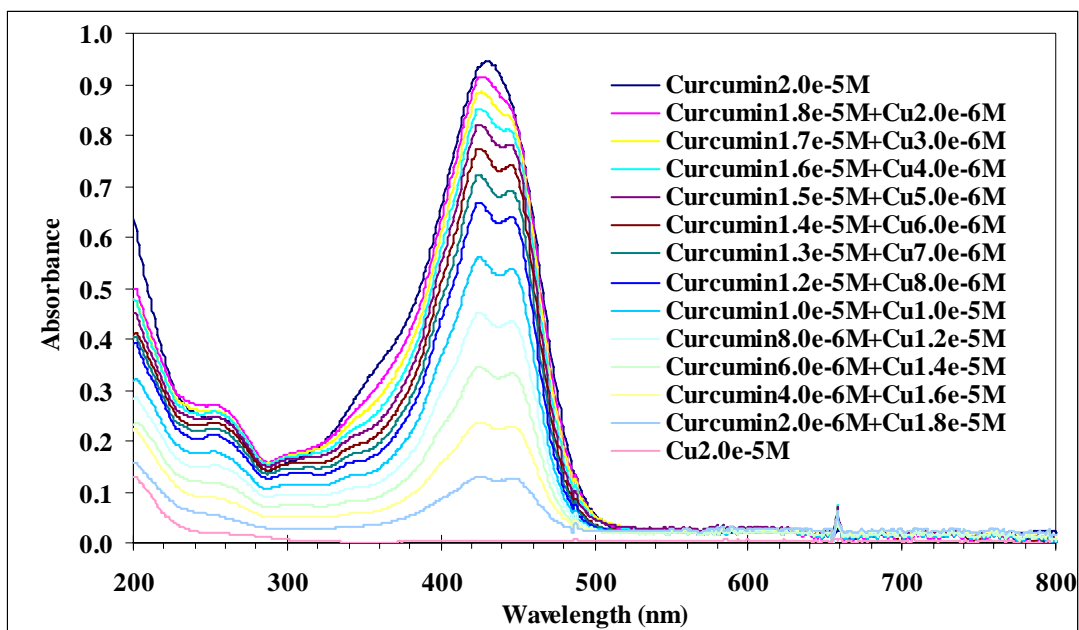


**Figure 56** UV-Vis spectra of the continuous variation method for curcumin-Cu(II) system

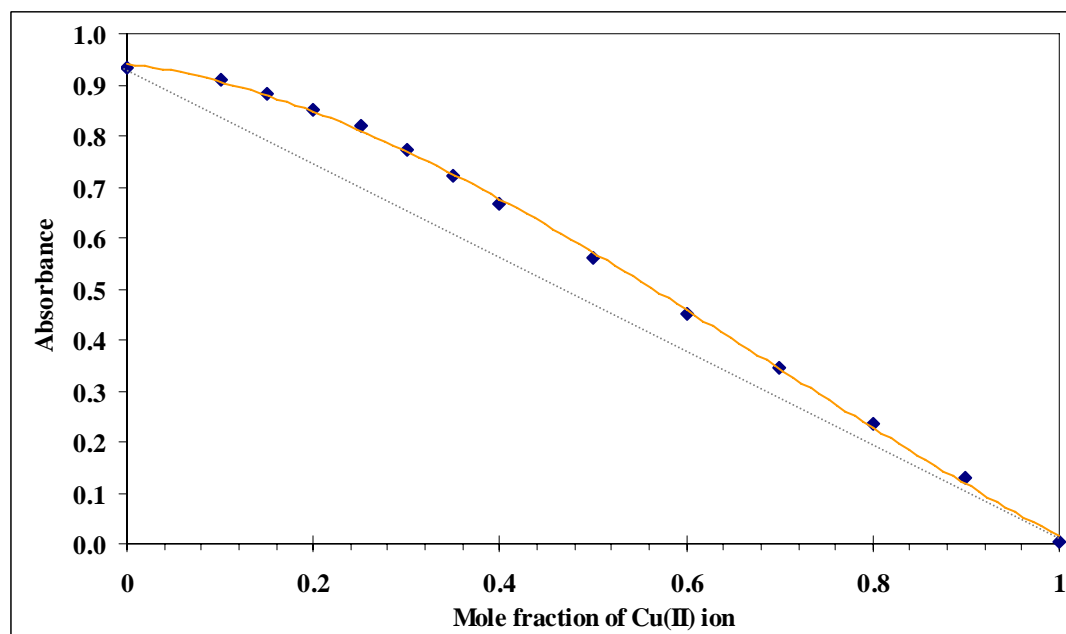


**Figure 57** Continuous variation plot of absorbance at 423 nm versus mole fraction of Cu(II) ion



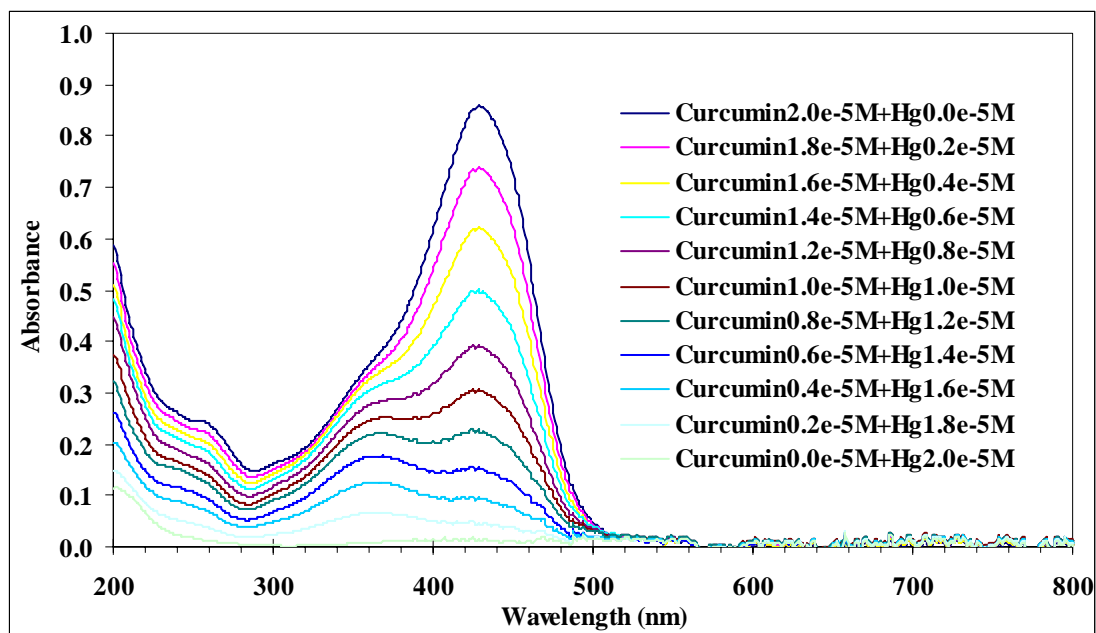


**Figure 58** UV-Vis spectra of the continuous variation method for curcumin-Hg(II) system

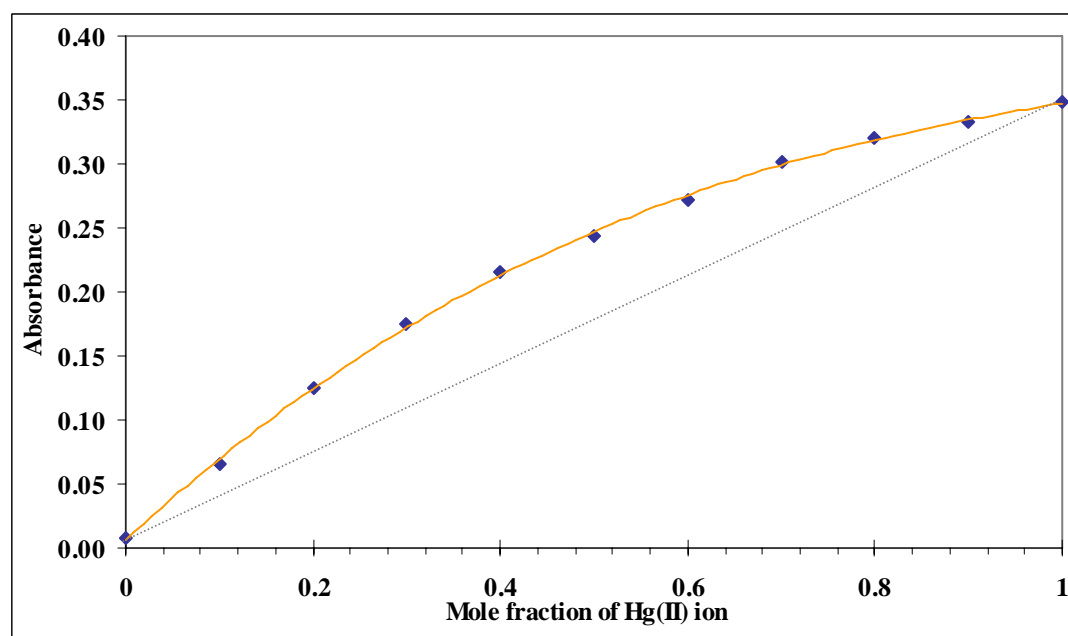


**Figure 59** Continuous variation plot of absorbance at 358 nm versus mole fraction of Hg(II) ion

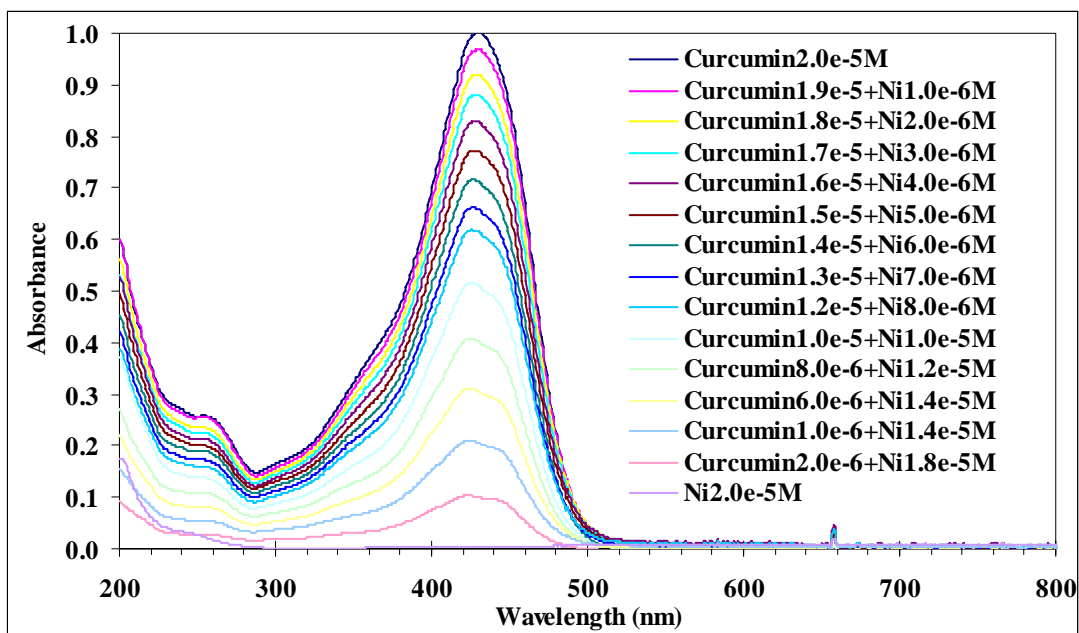


**Figure 60** UV-Vis spectra of the continuous variation method for curcumin-Ni(II) system

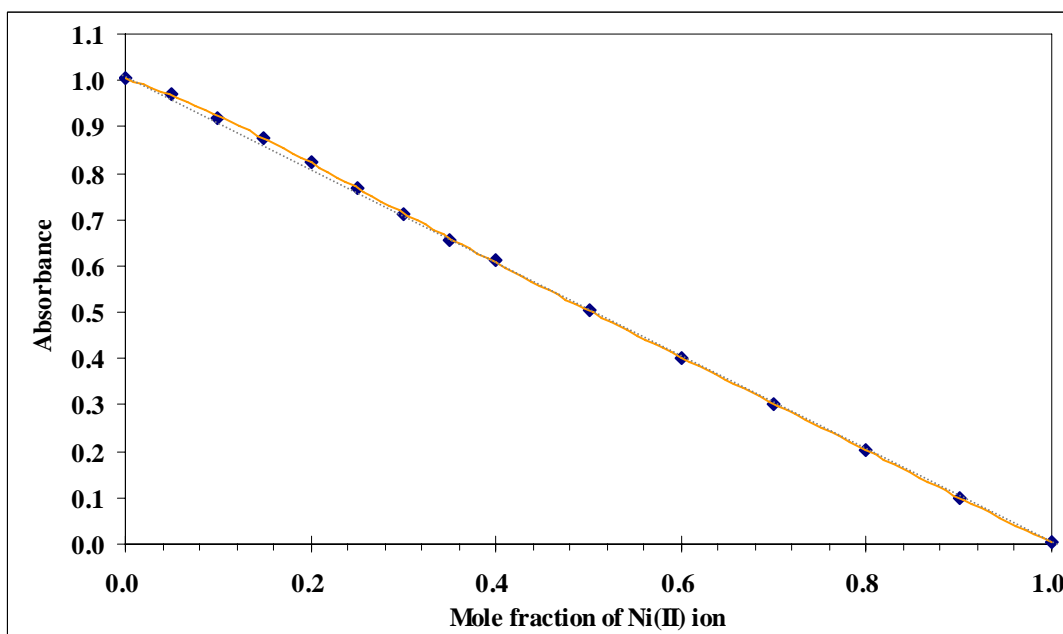


**Figure 61** Continuous variation plot of absorbance at 423 nm versus mole fraction of Ni(II) ion

The Job plot of these curcumin-metal systems do not give any inflection or parabolic portions so the stoichiometric ratio of the complexes cannot be determined by continuous variation method.

### 3.2.4 Study on the stoichiometry of curcumin-Cu(II), curcumin-Hg(II), curcumin-Ni(II) complexes by the continuous variation method after subtracted the residual free curcumin

The spectrophotometric data of curcumin-Cu, curcumin-Hg(II), and curcumin-Ni(II) in 3.2.3 were numerically subtracted by the unreacted curcumin and are shown in Figure 62, 64, and 66, respectively. Moreover, the Job's plots of them are illustrated in Figure 63, 65, and 67 respectively.

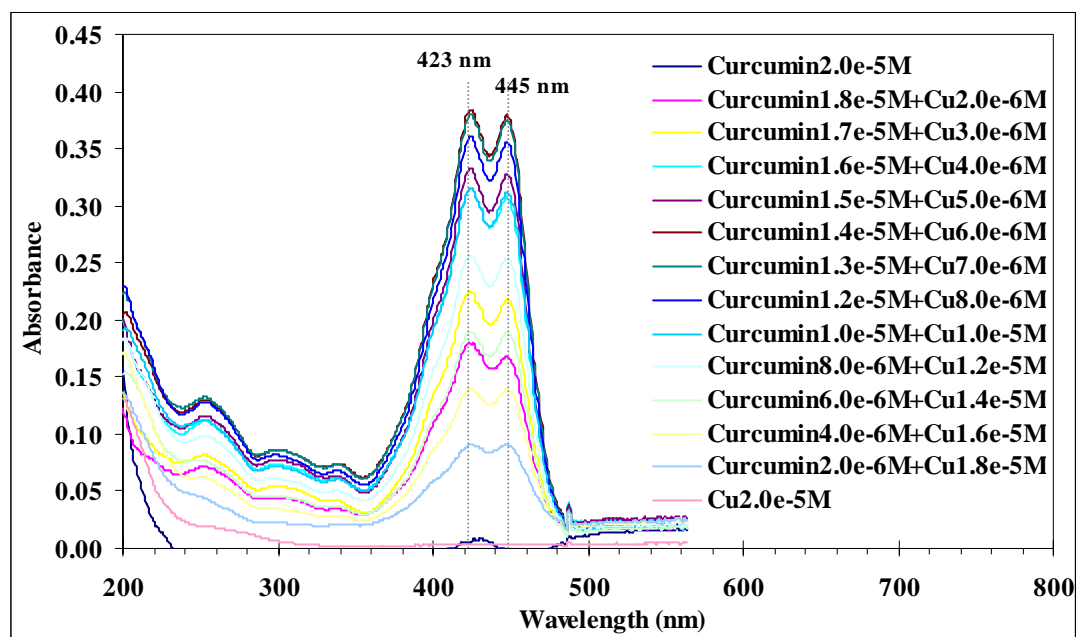


**Figure 62** UV-Vis spectra of continuous variation method for the curcumin-Cu(II) system (after subtracted free residual curcumin from Figure 56)

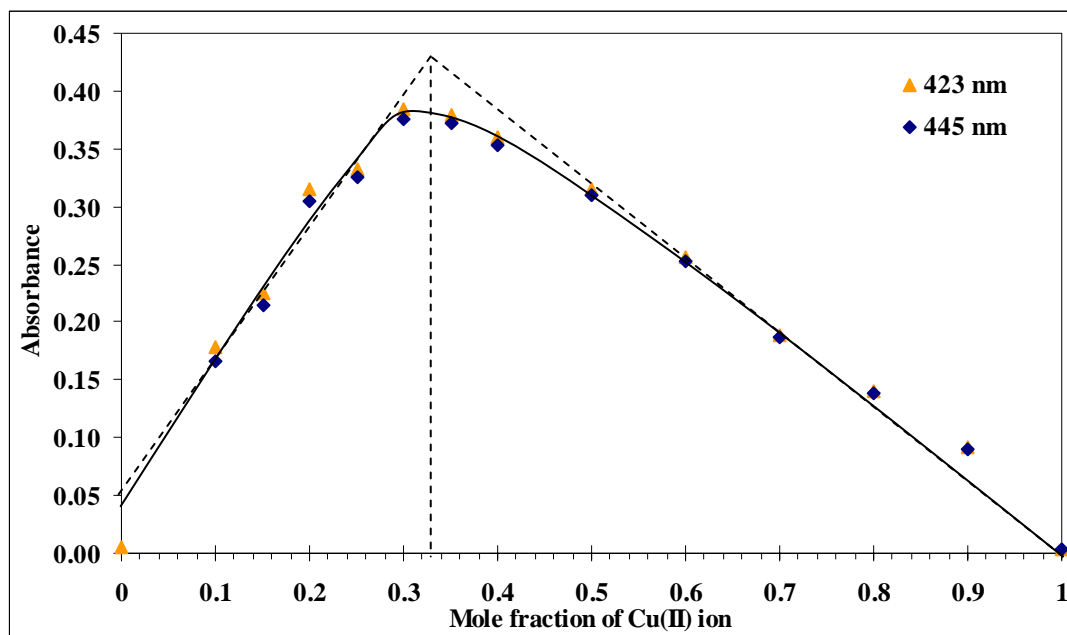


**Figure 63** Continuous variation plot of absorbance at 423 and 445 nm versus mole fraction of Cu(II) ion from Figure 62 (see Figure 57 for comparison)

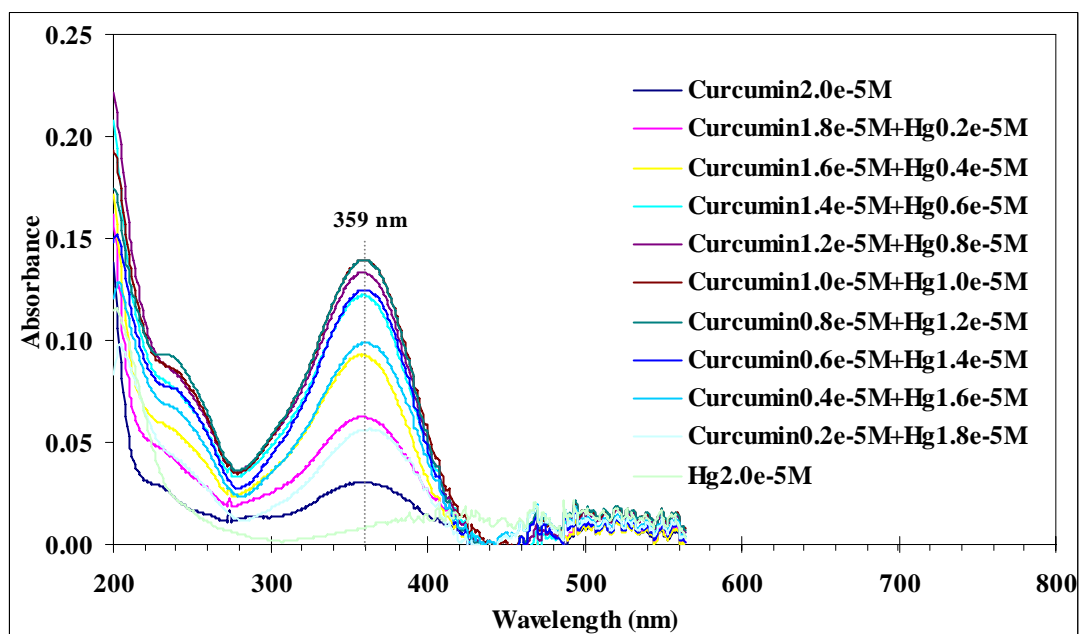


**Figure 64** UV-Vis spectra of continuous variation method for the curcumin-Hg(II) system (after subtracted free residual curcumin from Figure 58)

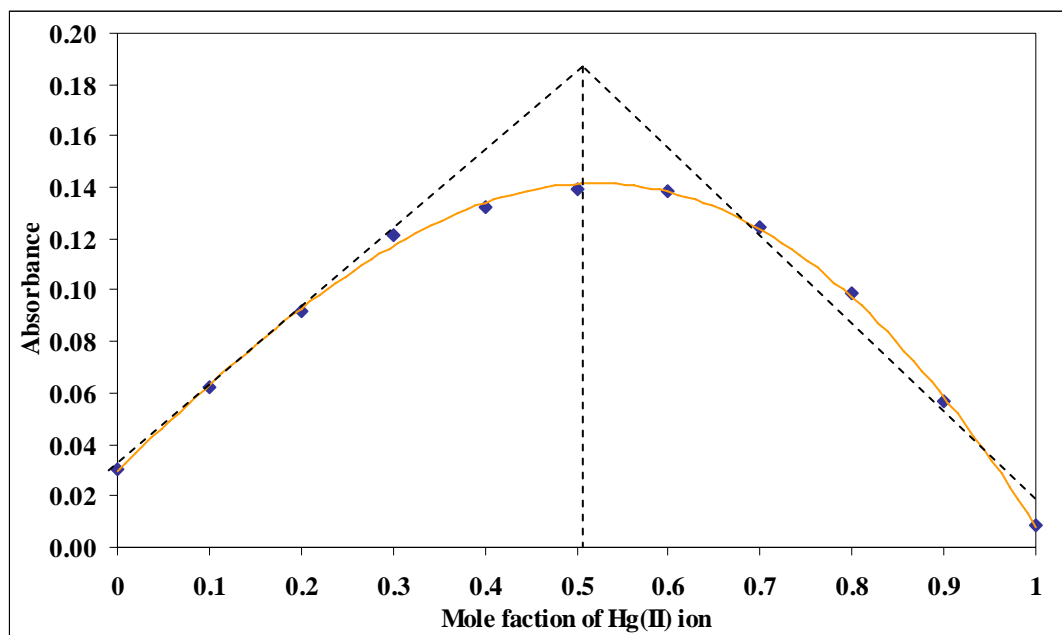


**Figure 65** Continuous variation plot of absorbance at 359 nm versus mole fraction of Hg(II) ion from Figure 64 (see Figure 59 for comparison)

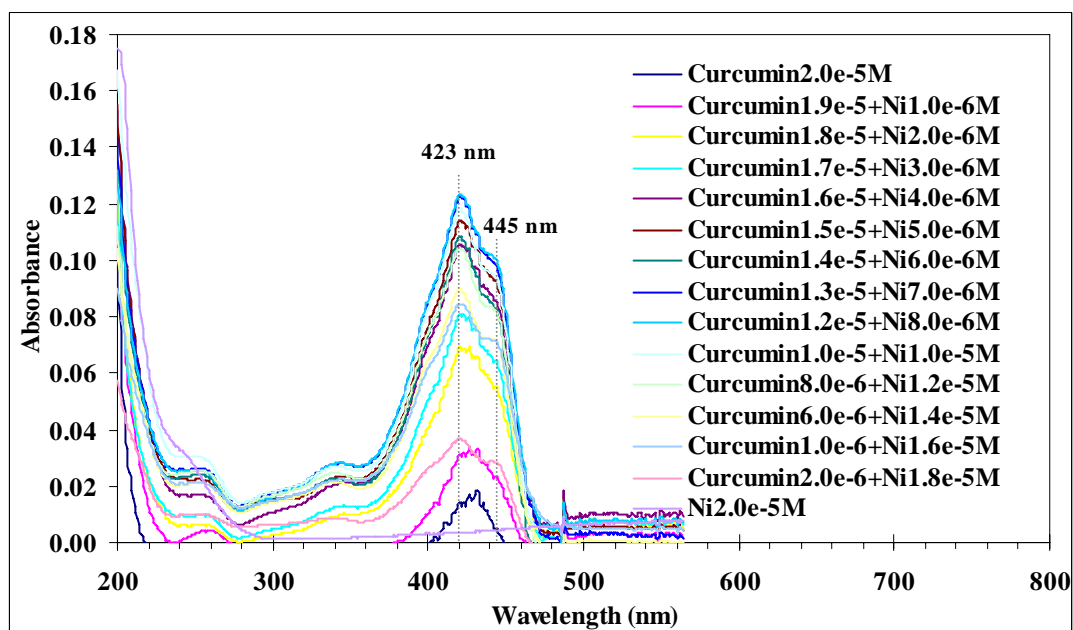


**Figure 66** UV-Vis spectra of continuous variation method for the curcumin-Ni(II) system (after subtracted free residual curcumin from Figure 65)

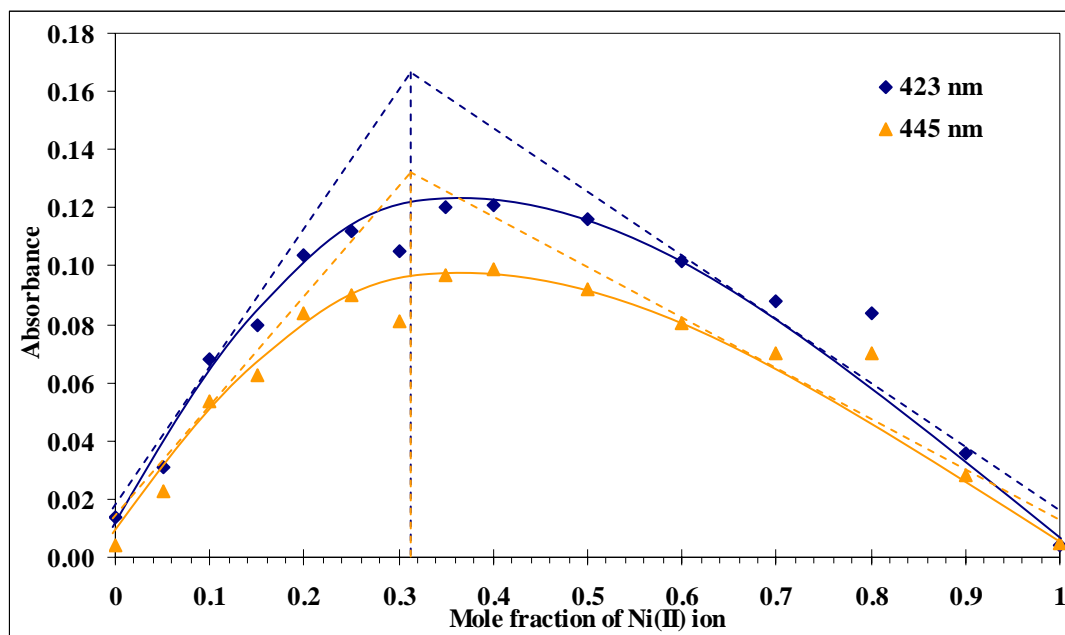


**Figure 67** Continuous variation plot of absorbance at 423 and 445 nm versus mole fraction of Ni(II) ion from Figure 66 (see Figure 61 for comparison)

After subtraction the residual free curcumin, the Job's plot of curcumin-Cu(II) and curcumin-Ni(II) gave an inflections portion, and the interception of two linear portions gave the mole fraction of metal ions at 0.33 and 0.32 which corresponded to the stoichiometric ratio of curcumin-Cu(II) and curcumin-Ni(II) as 2 : 1 composition. The Job's plot of curcumin-Hg(II) was a parabolic shape with the intersection value at mole fraction 0.52 corresponded to the stoichiometric ratio of curcumin-Hg(II) as 1 : 1 composition.

### 3.3 Studying spectra of curcumin analogous

To study the binding site of curcumin, curcumin analogous such as acetylacetone, ferulic acid, and vanillin, were studied to compare the reaction pattern with curcumin. The spectra of ferulic acid when added with Cu(II), Hg(II), and Ni(II) are shown in Figures 68-70, and likewise for vanillin and acetylacetone in Figures 71-73 and Figures 74-76.

#### 3.3.1 Ferulic acid

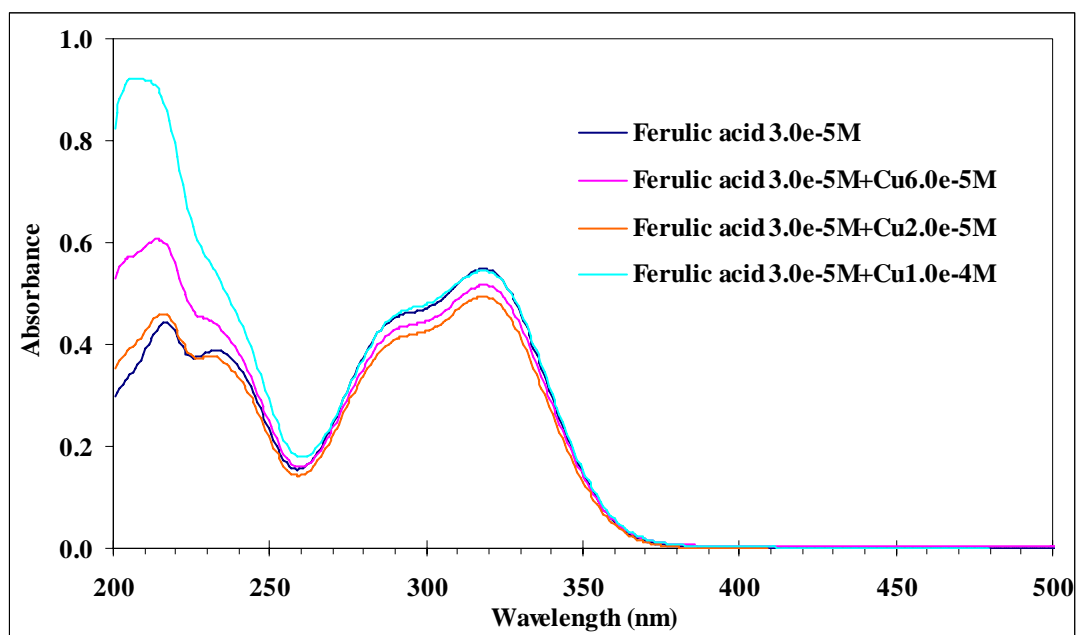


**Figure 68** Changes in absorption spectra of ferulic acid when added with Cu(II) ion

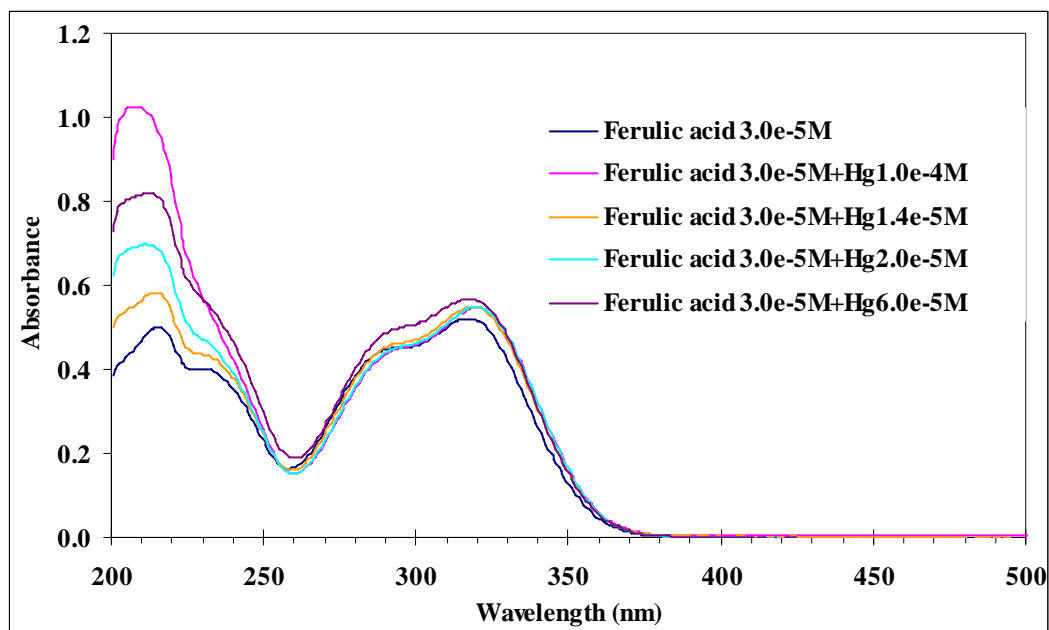


**Figure 69** Changes in absorption spectra of ferulic acid when added with Hg(II) ion

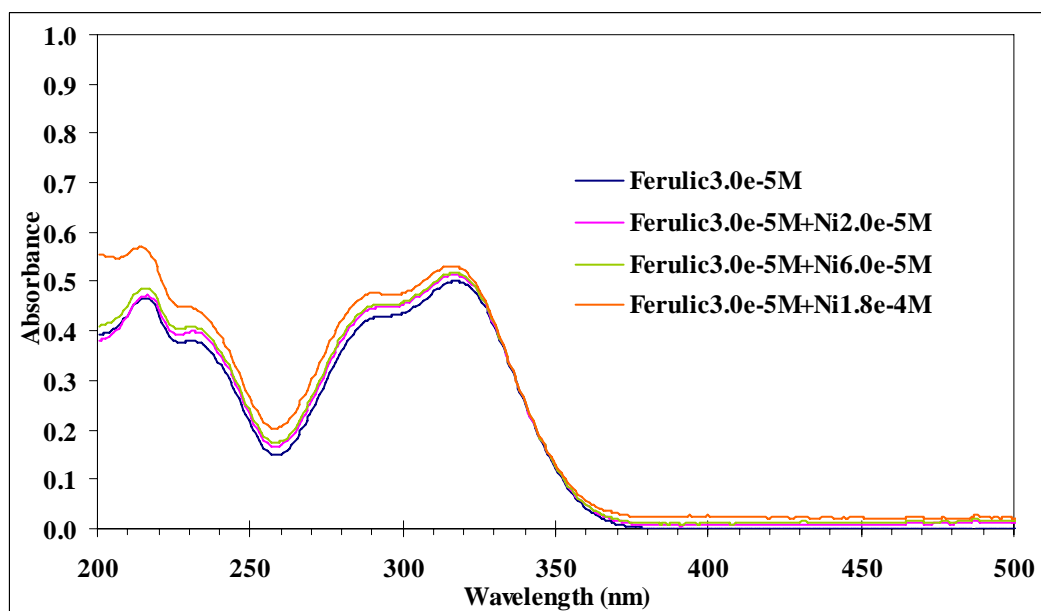


**Figure 70** Changes in absorption spectra of ferulic acid when added with Ni(II) ion



### 3.3.2 Vanillin

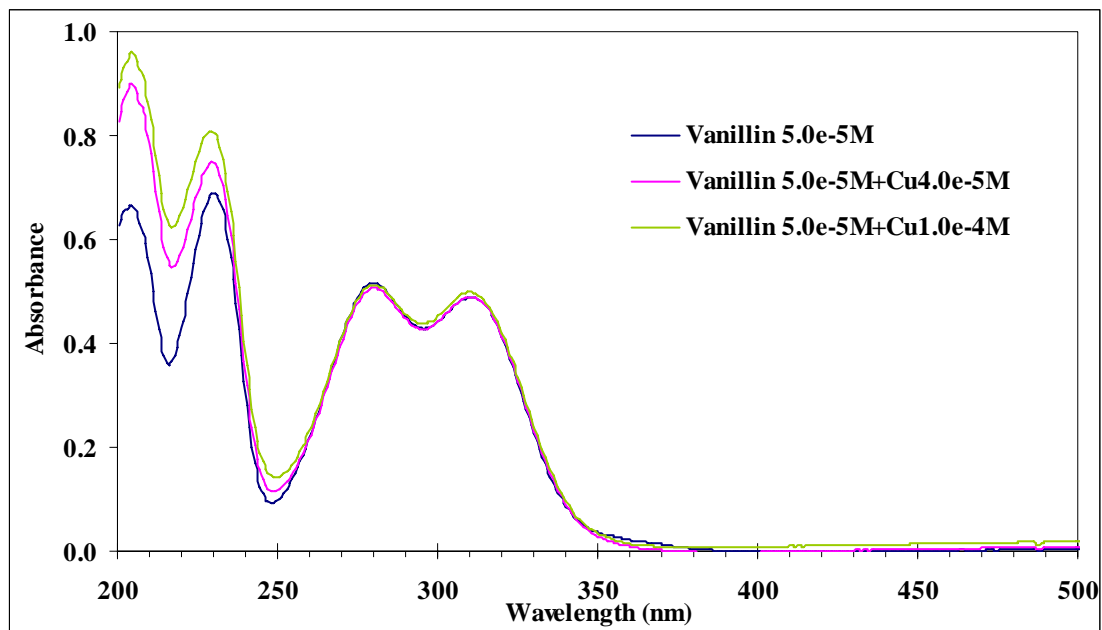


**Figure 71** Changes in absorption spectra of vanillin when added with Cu(II) ion

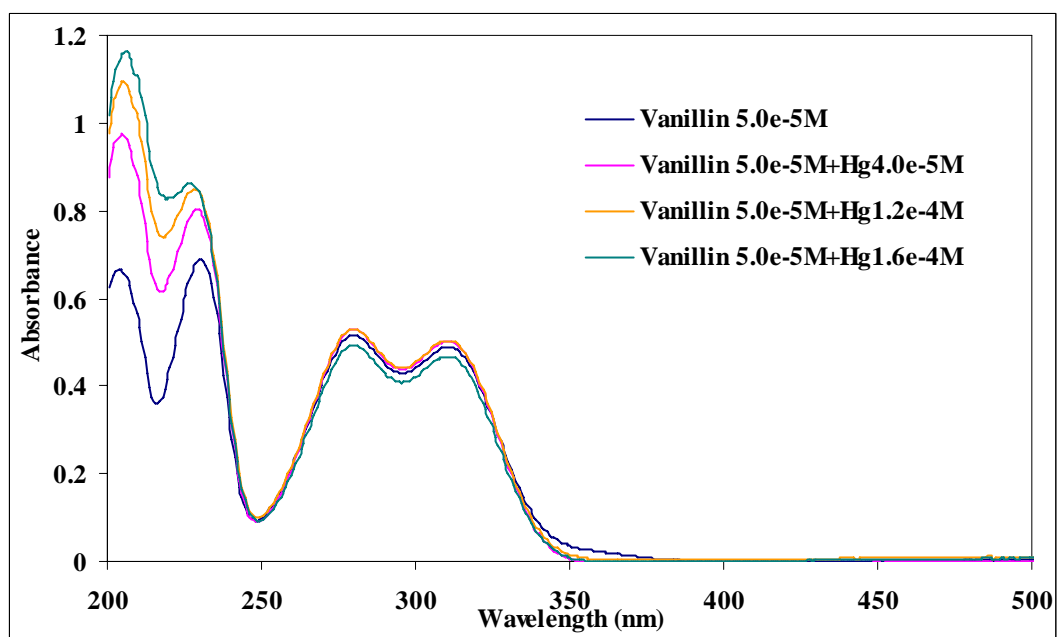


**Figure 72** Changes in absorption spectra of vanillin when added with Hg(II) ion

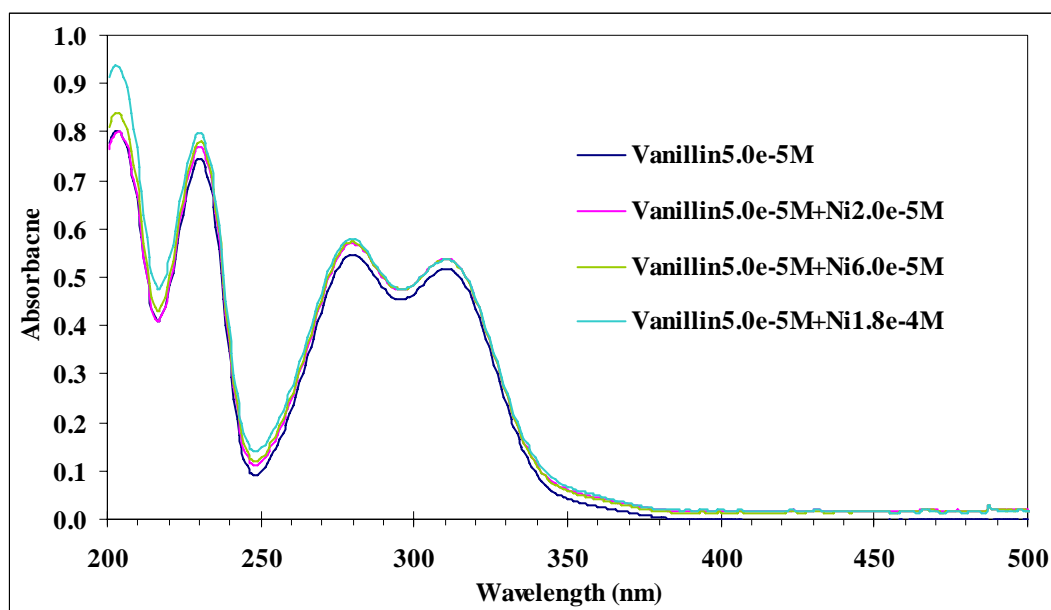


**Figure 73** Changes in absorption spectra of vanillin when added with Ni(II) ion

### 3.3.3 Acetylacetonone

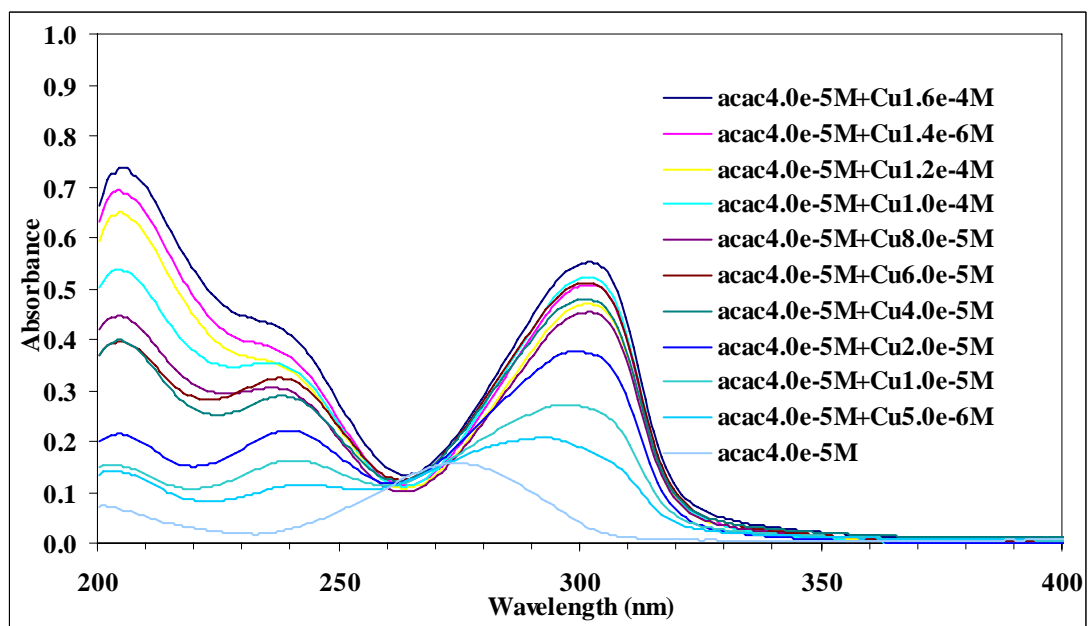


**Figure 74** Changes in absorption spectra of acetylacetonone when added with Cu(II) ion

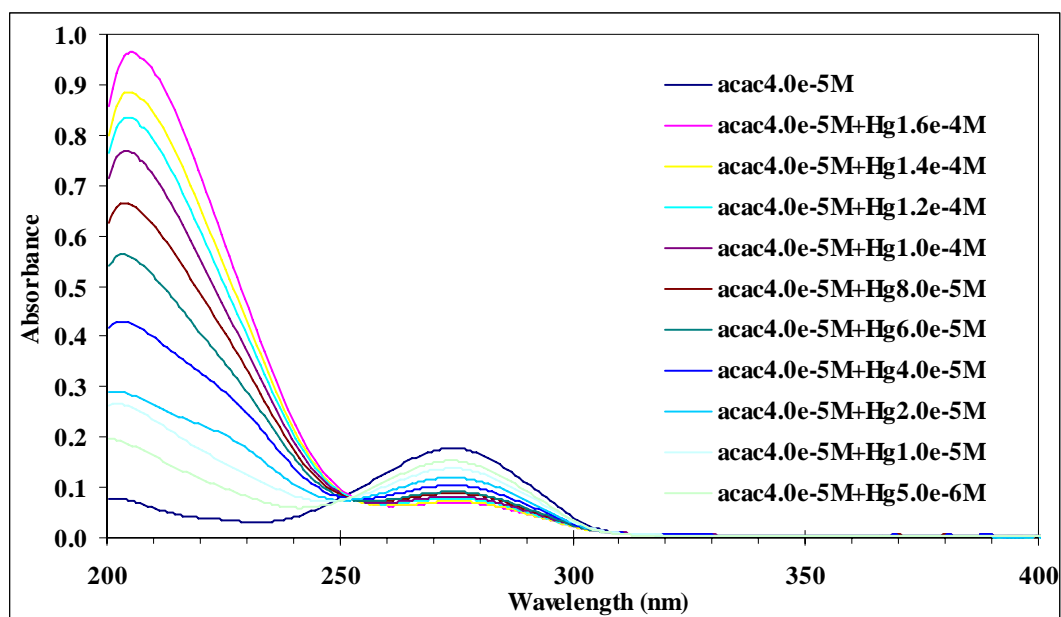


**Figure 75** Changes in absorption spectra of acetylacetonate when added with Hg(II) ion

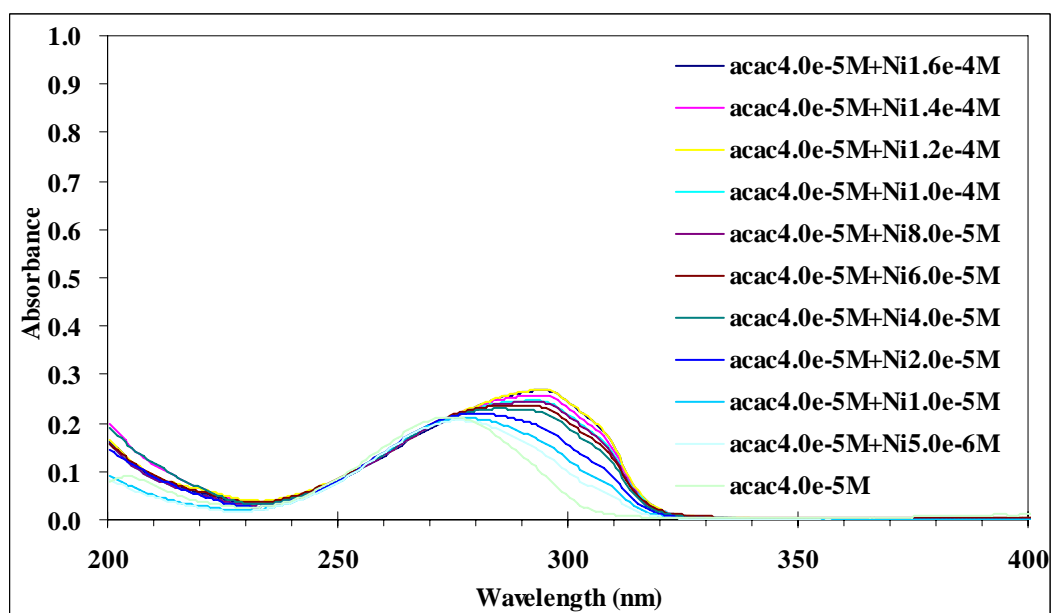


**Figure 76** Changes in absorption spectra of acetylacetonate when added with Ni(II) ion

Changes in acetylacetonate absorption pattern were clearly seen with the addition of Cu(II), Hg(II), and Ni(II) ions, while ferulic acid and vanillin absorption patterns did not show any obvious changes.

### 3.4 Complex formation constant

#### 3.4.1 For the 1:1 complex

##### 3.4.1.1 Curcumin-Hg(II)

The complex formation constant ( $K$ ) of curcumin-Hg(II) complex was calculated by using Eq. (2). From the mole ratio data the  $K$  value could be calculated by using the composition at equilibrium (Table 13) which came out as  $4.02 \times 10^4$  or  $\log K = 4.60$ .

**Table 13** The composition of curcumin-Hg(II) system from the mole-ratio method

Absorbance 359 nm	Initial concentration, M		Final concentration, M		
	Curcumin	Hg	Free curcumin	Complex	Hg
1.03577	$2.00 \times 10^{-5}$	0	$2.07 \times 10^{-5}$	-	-
0.825317	$2.00 \times 10^{-5}$	$5.00 \times 10^{-6}$	$1.65 \times 10^{-5}$	$3.50 \times 10^{-6}$	$1.50 \times 10^{-6}$
0.789927	$2.00 \times 10^{-5}$	$6.70 \times 10^{-5}$	$1.57 \times 10^{-5}$	$4.30 \times 10^{-6}$	$2.40 \times 10^{-6}$
0.759751	$2.00 \times 10^{-5}$	$1.00 \times 10^{-5}$	$1.51 \times 10^{-5}$	$4.90 \times 10^{-6}$	$5.10 \times 10^{-6}$
<b>0.671828*</b>	<b><math>2.00 \times 10^{-5}</math></b>	<b><math>2.00 \times 10^{-5}</math></b>	<b><math>1.31 \times 10^{-5}</math></b>	<b><math>6.90 \times 10^{-6}</math></b>	<b><math>1.31 \times 10^{-5}</math></b>
0.610352	$2.00 \times 10^{-5}$	$4.00 \times 10^{-5}$	$1.19 \times 10^{-5}$	$8.10 \times 10^{-6}$	$3.19 \times 10^{-5}$
0.569907	$2.00 \times 10^{-5}$	$6.00 \times 10^{-5}$	$1.09 \times 10^{-5}$	$9.10 \times 10^{-6}$	$5.09 \times 10^{-5}$
0.5179	$2.00 \times 10^{-5}$	$8.00 \times 10^{-5}$	$1.00 \times 10^{-5}$	$1.00 \times 10^{-5}$	$7.00 \times 10^{-5}$
0.494291	$2.00 \times 10^{-5}$	$1.00 \times 10^{-4}$	$9.40 \times 10^{-6}$	$1.06 \times 10^{-5}$	$8.94 \times 10^{-5}$
0.487303	$2.00 \times 10^{-5}$	$1.20 \times 10^{-4}$	$9.20 \times 10^{-6}$	$1.08 \times 10^{-5}$	$1.09 \times 10^{-4}$
0.493138	$2.00 \times 10^{-5}$	$1.40 \times 10^{-4}$	$9.20 \times 10^{-6}$	$1.08 \times 10^{-5}$	$1.29 \times 10^{-4}$
0.453434	$2.00 \times 10^{-5}$	$1.60 \times 10^{-4}$	$8.50 \times 10^{-6}$	$1.15 \times 10^{-5}$	$1.49 \times 10^{-4}$
0.463428	$2.00 \times 10^{-5}$	$1.80 \times 10^{-4}$	$8.50 \times 10^{-6}$	$1.15 \times 10^{-5}$	$1.69 \times 10^{-4}$

\* equilibrium

The  $K$  value was also calculated by using the Benesi-Hildebrand equation (Eq. 15) where  $C_{Cur}C_{Hg}/A$  was plotted against  $C_{Hg}$ . In this plot, the 1:1 complex would yield a straight line which  $K = (\text{slope})/(\text{intercept})$  and  $\varepsilon = 1/(\text{slope})$ . The resulting Benesi-Hildebrand plot is shown in Figure 77. From this plot,  $K = 6.67 \times 10^4$  or  $\log K = 4.82$  and  $\varepsilon = 25000$  or  $\log \varepsilon = 4.40$ .

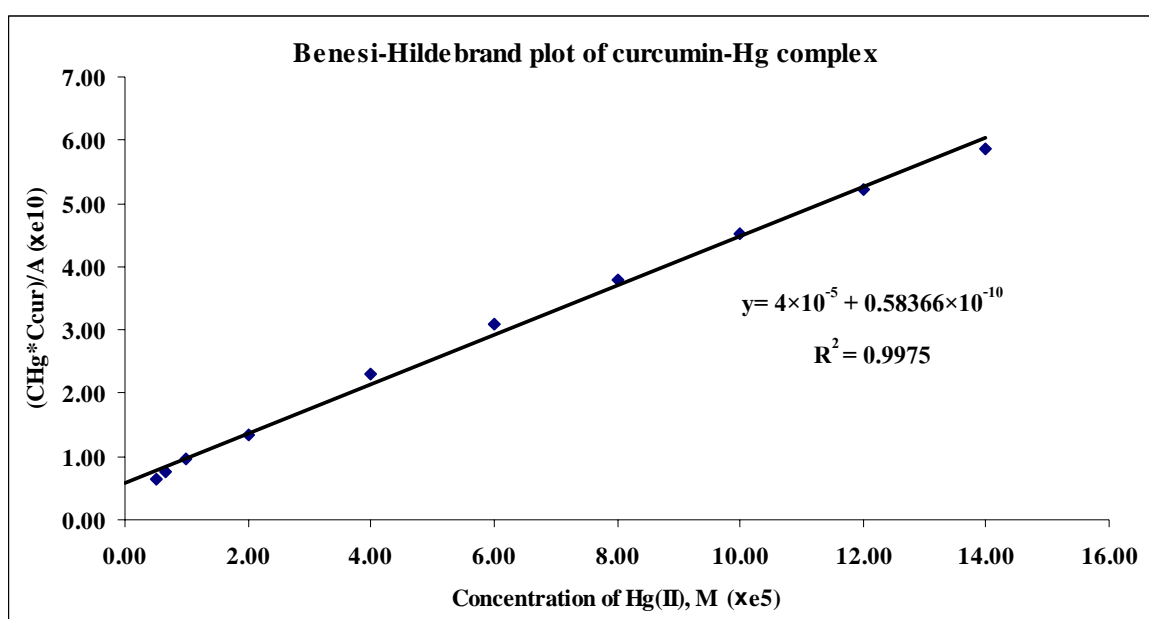


**Figure 77** The Benesi-Hildebrand plot

### 3.4.2 For the 2:1 complex

#### 3.4.2.1 Curcumin-Cu(II)

The complex formation constant ( $\beta$ ) of curcumin-Cu(II) complex was calculated by using Eq. (2). From the mole ratio data the  $\beta$  value could be calculated by using the composition at equilibrium (Table 14) which came out as  $6.76 \times 10^9$  or  $\log \beta = 9.80$ .

**Table 14** The composition of curcumin-Cu(II) system from the mole-ratio method

Absorbance 424 nm	Initial concentration, M		Final concentration, M		
	Curcumin	Cu	Free curcumin	Complex	Cu
0.002331	$2.00 \times 10^{-5}$	0	$2.00 \times 10^{-5}$	-	-
0.177376	$2.00 \times 10^{-5}$	$2.00 \times 10^{-6}$	$1.70 \times 10^{-5}$	$1.50 \times 10^{-6}$	$5.00 \times 10^{-7}$
0.31577	$2.00 \times 10^{-5}$	$4.00 \times 10^{-6}$	$1.50 \times 10^{-5}$	$2.50 \times 10^{-6}$	$1.50 \times 10^{-6}$
0.435048	$2.00 \times 10^{-5}$	$6.00 \times 10^{-6}$	$1.30 \times 10^{-5}$	$3.50 \times 10^{-6}$	$2.50 \times 10^{-6}$
0.504902	$2.00 \times 10^{-5}$	$8.00 \times 10^{-6}$	$1.20 \times 10^{-5}$	$4.00 \times 10^{-6}$	$4.00 \times 10^{-6}$
<b>0.563686*</b>	<b><math>2.00 \times 10^{-5}</math></b>	<b><math>1.00 \times 10^{-5}</math></b>	<b><math>1.10 \times 10^{-5}</math></b>	<b><math>4.50 \times 10^{-6}</math></b>	<b><math>5.50 \times 10^{-6}</math></b>
0.566976	$2.00 \times 10^{-5}$	$1.50 \times 10^{-5}$	$1.10 \times 10^{-5}$	$4.50 \times 10^{-6}$	$1.05 \times 10^{-5}$
0.577686	$2.00 \times 10^{-5}$	$2.00 \times 10^{-5}$	$1.10 \times 10^{-5}$	$4.50 \times 10^{-6}$	$1.55 \times 10^{-5}$
0.578416	$2.00 \times 10^{-5}$	$3.00 \times 10^{-5}$	$1.10 \times 10^{-5}$	$4.50 \times 10^{-6}$	$2.55 \times 10^{-5}$
0.572656	$2.00 \times 10^{-5}$	$4.00 \times 10^{-5}$	$1.10 \times 10^{-5}$	$4.50 \times 10^{-6}$	$3.55 \times 10^{-5}$

\* equilibrium

### 3.4.2.2 Curcumin-Ni(II)

The complex formation constant ( $\beta$ ) of curcumin-Ni complex was calculated by using Eq. (2). From the mole ratio data the  $\beta$  value could be calculated by using the composition at equilibrium (Table 15) which came out as  $6.75 \times 10^9$  or  $\log \beta = 8.83$

**Table 15** The composition of curcumin-Ni(II) system from the mole-ratio method

Absorbance 420 nm	Initial concentration, M		Final concentration, M		
	Curcumin	Ni	Free curcumin	Complex	Ni
0.014154	$2.00 \times 10^{-5}$	0	$2.00 \times 10^{-5}$	-	-
0.086083	$2.00 \times 10^{-5}$	$2.00 \times 10^{-6}$	$1.90 \times 10^{-5}$	$5.00 \times 10^{-7}$	$1.50 \times 10^{-6}$
0.124894	$2.00 \times 10^{-5}$	$4.00 \times 10^{-6}$	$1.82 \times 10^{-5}$	$9.00 \times 10^{-7}$	$3.10 \times 10^{-6}$
0.137341	$2.00 \times 10^{-5}$	$6.00 \times 10^{-6}$	$1.80 \times 10^{-5}$	$1.00 \times 10^{-6}$	$5.0 \times 10^{-6}$
0.175539	$2.00 \times 10^{-5}$	$8.00 \times 10^{-6}$	$1.75 \times 10^{-5}$	$1.25 \times 10^{-6}$	$6.75 \times 10^{-6}$
<b>0.215694*</b>	<b><math>2.00 \times 10^{-5}</math></b>	<b><math>1.00 \times 10^{-5}</math></b>	<b><math>1.68 \times 10^{-5}</math></b>	<b><math>1.60 \times 10^{-6}</math></b>	<b><math>8.40 \times 10^{-6}</math></b>
0.257482	$2.00 \times 10^{-5}$	$1.50 \times 10^{-5}$	$1.60 \times 10^{-5}$	$2.00 \times 10^{-6}$	$1.3 \times 10^{-5}$
0.290039	$2.00 \times 10^{-5}$	$2.00 \times 10^{-5}$	$1.55 \times 10^{-5}$	$2.25 \times 10^{-6}$	$1.78 \times 10^{-5}$
0.331947	$2.00 \times 10^{-5}$	$3.00 \times 10^{-5}$	$1.47 \times 10^{-5}$	$2.65 \times 10^{-6}$	$2.74 \times 10^{-5}$
0.389755	$2.00 \times 10^{-5}$	$4.00 \times 10^{-5}$	$1.35 \times 10^{-5}$	$3.25 \times 10^{-6}$	$3.68 \times 10^{-5}$

\* equilibrium

### 3.5 Trends of pH changes for curcumin-metal system (with Cu(II), Ni(II), and Hg(II))

The pH of curcumin solutions were recorded after the metal ion solution was added. The trends of pH with added metal ions (Cu(II), Hg(II), and Ni(II)) were plotted against the concentrations of the metal ion added are shown in Figures. 78-80. The pH of the systems was decreased about 1 pH from the pH of curcumin alone after added the metal ion solutions.

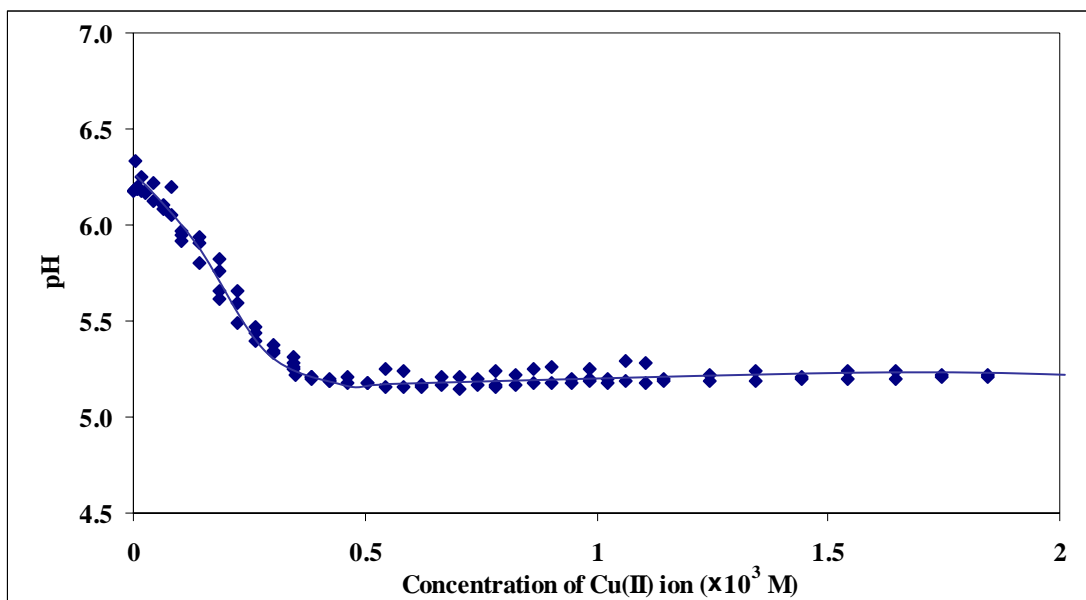


**Figure 78** pH of curcumin solution when added Cu(II) solution



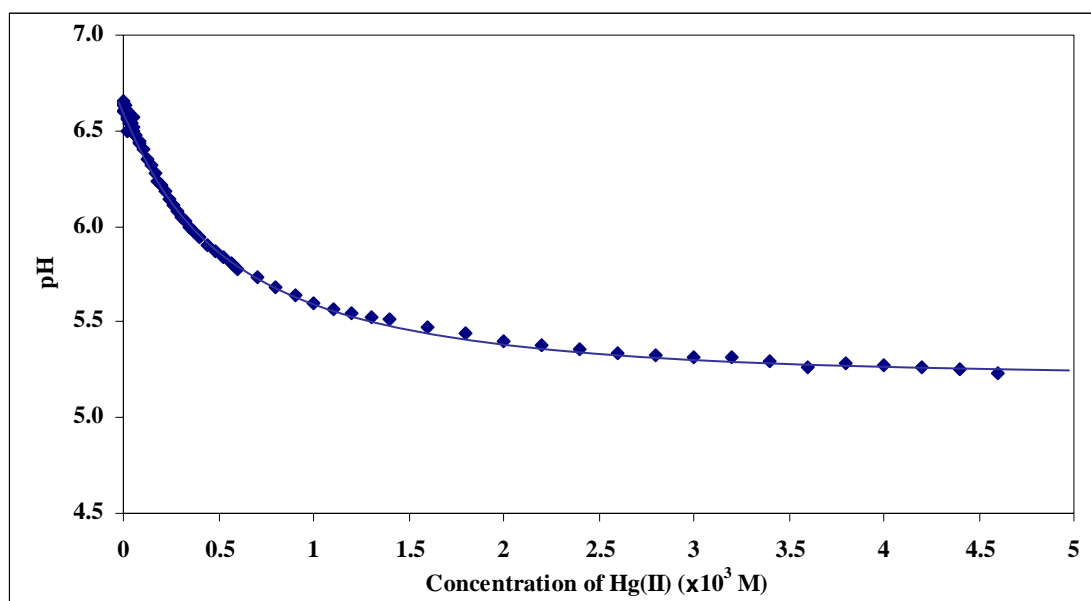


**Figure 79** pH of curcumin solution when added Hg(II) solution

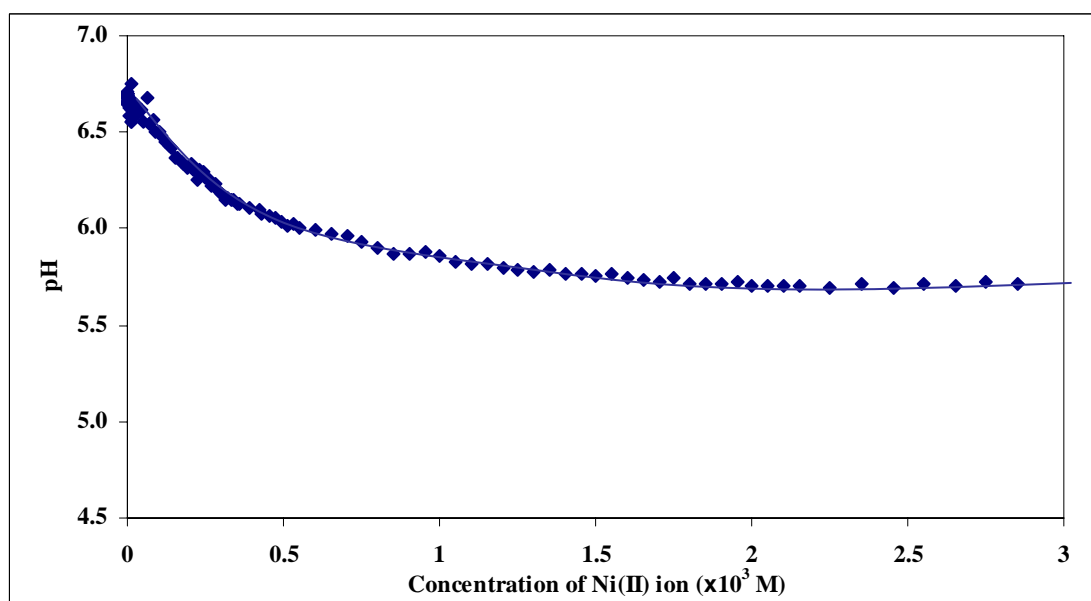


**Figure 80** pH of curcumin solution when added Ni(II) solution